Water Resources Research

RESEARCH ARTICLE
10.1029/2017WR021825

Key Points:
- Groundwater and streamflow ages differ at the well-studied Maimai watershed in New Zealand
- Volumetric contributions of old bedrock groundwater to runoff generation were limited by low bedrock permeability
- Catchment storage was dominated by two distinct and contrasting components: shallow, young soil water and deep, and much older bedrock water

Supporting Information:
- Supporting Information S1

Correspondence to:
C. P. Gabrielli,
chris.gabrielli@usask.ca

Citation:
Gabrielli, C. P., Morgenstern, U., Stewart, M. K., & McDonnell, J. J. (2018). Contrasting groundwater and streamflow ages at the Maimai watershed. *Water Resources Research*, *54*, 3937–3957. https://doi.org/10.1029/2017WR021825

Received 14 SEP 2017
Accepted 29 APR 2018
Accepted article online 7 MAY 2018
Published online 8 JUN 2018

Contrasting Groundwater and Streamflow Ages at the Maimai Watershed

C. P. Gabrielli[1], U. Morgenstern[2], M. K. Stewart[3], and J. J. McDonnell[1]

[1]Global Institute for Water Security, University of Saskatchewan, Saskatoon, SK, Canada, [2]GNS Science, Lower Hutt, New Zealand, [3]Aquifer Dynamics & GNS Science, Lower Hutt, New Zealand

Abstract Understanding the links between groundwater age, runoff generation processes, and their effects on stream water transit time (TT) is a major research challenge. Here we present new tritium age dating and hydrogeological characterization from 40 bedrock wells drilled at the intensively studied Maimai Experimental Watershed in New Zealand. We investigated the extent, dynamics, and age of the groundwater in a 4.5 ha headwater catchment over a 400 day period. In particular, we explored the controls of bedrock structure on aquifer dynamics, the aquifer flow domain and its influence on time-varying stream water TT. We show that low permeability hillslope bedrock minimizes deep recharge, thereby regulating groundwater age, stream water MTT, and surface water-groundwater interaction. Two distinct hydrologic units can represent catchment storage: shallow young soil storage and deep much older bedrock groundwater. Groundwater ages near discharge zones were up to 23 years compared to soil water ages that ranged between 0.1 and 0.5 years. This difference in age for the two main storages resulted in contrasting seasonal stream water TT response. During the 8 month wet season, stream water TT was young and stable while stream water TT in the slightly drier summer season was highly dynamic. These qualitative field observations are a process exemplar that support the Berghuijs and Kirchner (2017) quantitative descriptions of preferential release of young streamflow; and for the Maimai catchment, support the notion that most groundwater is exchanged only slowly with the surface and is therefore relatively old.

1. Introduction

Headwater catchments are the building blocks of the hydrologic landscape and thus control the downstream flux of water, nutrients, and solutes to their parent watersheds. Understanding how and across what time scales these uplands catchments store and ultimately release their water is necessary for effective resource management, especially under changing climate regimes (Stocker, 2014) and ever increasing demands on groundwater resources (Wada et al., 2010). While much new discovery continues on different components of the headwater catchment water balance (Brooks et al., 2010; Overeem et al., 2013) and runoff generation processes (Penna et al., 2015; Soulsby et al., 2015), deep catchment storage dynamics have received less attention. Catchment storage is a primary control of both discharge dynamics and subsurface mixing processes (Creutzfeldt et al., 2014; Kirchner, 2009; Seibert et al., 2003), yet headwater storage changes within bedrock remains poorly characterized (McNamara et al., 2011). In particular, the contribution of bedrock groundwater to the storage-discharge relationship is difficult to understand and assess, and, as a result, total catchment storage is still largely unknown in most research sites (Pfister et al., 2017; Sayama et al., 2011).

Base flow recession analysis (Wittenberg & Sivapalan, 1999) and GRACE-based (Creutzfeldt et al., 2014; Sproles et al., 2015) methods have provided insights into catchment scale storage-discharge relationships, however, these black-box approaches fail to resolve internal processes, structures, and patterns—information necessary to drive the next generation of catchment scale models (McMillan et al., 2011). Further, recent increases in computational power have led to impressive new simulations of groundwater contributions to streamflow in headwater catchments (Ebel & Loague, 2006; Maxwell & Condon, 2016). But while these and other simulations are informative, much basic field work is still needed to age-date and understand bedrock groundwater flow processes in headwater catchments and to quantify its link to, and influence on, streamflow characteristics. Indeed, the influence of bedrock as an additional storage volume (beyond that of the soil mantle) remains a significant source of uncertainty, and until only recently, has rock-moisture been identified as a critical headwater reservoir for both runoff generation and plant water use (Rempe & Dietrich, 2018).

Bedrock poses a unique challenge to headwater process investigations: the logistical difficulties associated with gaining access into bedrock in steep, remote, and often roadless terrain combined with complex fracture-dominated flow paths have historically thwarted attempts to study bedrock flow path dynamics directly (Asano et al., 2009; Asano & Uchida, 2012; Katsuyama et al., 2010; MacDonald, 1988; Millares et al., 2009; Uchida & Asano, 2010). Geophysical techniques offer a promising way forward (Binley et al., 2010); however, interpretation of results are often ambiguous without significant ground truthing. Recent advancements in mobile drilling technology (Gabrielli & McDonnell, 2012) make the direct observation of bedrock groundwater dynamics in difficult-to-access headwater catchments more readily available. But there exists only a limited number of studies which have gained full access to, and provided complete characterization of, bedrock groundwater in the headwaters. Most previous investigations have been constrained to the hillslope scale (Anderson et al., 1997; Gabrielli et al., 2012; Masaoka et al., 2016; Montgomery et al., 1997; Onda et al., 2001) or to using bedrock-spring discharge as a proxy for deeper bedrock groundwater dynamics (Asano et al., 2002; Onda et al., 2001; Uchida et al., 2002).

Recent theoretical work has provided a quantitative framework to describe the influence of subsurface heterogeneity and permeability contrasts on the age difference between water stored in catchments and the water released by catchments (Berghuijs & Kirchner, 2017). Yet, to date, we lack the integrated field measurements to test this theory and to provide site-based understanding of bedrock characteristics, their control on the bedrock groundwater flow domain and how these characteristics affect groundwater dynamics, age, and surface water-groundwater interactions across varying catchment wetness conditions. As interest in the connection between shallow and deeper critical zone processes grows (Jasechko et al., 2017; McDonnell, 2017; Riebe et al., 2017), these field descriptions are increasingly important.

Here we present new results from an intensive field campaign that combines hydrometric, geochemical, and tritium-based analyses with groundwater monitoring to characterize the underlying headwater bedrock aquifer and its connection and contribution to streamflow and stream water age. The overarching goal was to use field data to inform the relationship between groundwater and streamflow ages. We based our work at the well-studied Maimai watershed in New Zealand. Maimai is often viewed as an exemplar for how steep, wet catchments generate runoff (McGlynn et al., 2002)—yet, to date, little work has been done to characterize the bedrock groundwater at the site. The Maimai catchment is known for its flashy and responsive hydrograph, extremely high runoff ratios and young stream water discharge (Mosley, 1979; Pearce et al., 1986). For nearly 40 years, it has existed as a testing ground for hypothesis testing in hillslope hydrology, revealing insights on the mechanisms and timing of subsurface stormflow (Mosley, 1979; Pearce et al., 1986; Sklash et al., 1986), on mixing and effusion of old and new water (McDonnell, 1990) and on the spatial and time source components of runoff generation and its control on stream water chemistry (McGlynn et al., 2004; McGlynn & McDonnell, 2003).

We leverage the process hydrology of Maimai to examine the role of deep bedrock groundwater and its impact on flow and mean transit time (MTT) of stream water. We present new data from 40 wells down to ∼9 m, installed with a backpackable drill rig (modified from Gabrielli and McDonnell (2012)). We sampled them for groundwater tritium concentration and monitored water table dynamics for 400 days. Maimai stream water is some of the youngest documented in the isotope hydrology literature with MTT estimates on the order of only 4 months (Pearce et al., 1986). And to date, no direct observation of bedrock groundwater connectivity to the stream has been made.

Here we use the approach of Morgenstern et al. (2010) to translate groundwater tritium values into robust water ages and then relate this to the bedrock aquifer flow structure, groundwater dynamics, and stream water silica concentration to determine how it affects the time-varying stream water transit time. Specifically, we address the following research questions:

1. How do bedrock permeability patterns relate to headwater landscape position?
2. What are the spatial and temporal dynamics of bedrock groundwater?

3. How does permeability structure affect the age and spatial patterns of age within bedrock groundwater?
4. To what extent is bedrock groundwater connected to the stream and how does this influence time-varying stream water transit time?

Whilst focused on Maimai as a test case, these research questions are some of the most pressing research questions in process hydrology, as noted in recent reviews (Grant & Dietrich, 2017; McDonnell, 2017; McNamara et al., 2011; White et al., 2015).

2. Study Site

The 280 ha Maimai Experimental Watershed is located on the northwest coast of the South Island, New Zealand, in the Tawhai State Forest (Figure 1; 42°05′S 171°47′E). This work focused specifically on the 4.5 ha subwatershed known as M8 (the original site of work by Mosley (1979) and McDonnell (1990)). Elevation within M8 ranges from 251 to 348 m.a.s.l. The landscape is highly dissected and dominated by three main geomorphic landscape units: highly convergent and divergent hillslopes, steep ephemeral hollows, and a gently sloping riparian zone (Weiler et al., 2003). Hillslopes are short (<100 m) and steep (range: 15–65°, average: 34°).

Soils are thin, averaging 0.6 m deep with a range of 0.1–1.8 m, and highly transmissive (Brammer, 1996). The bedrock underlying the catchment is a conglomerate known as Old Man Gravel. It belongs to a larger

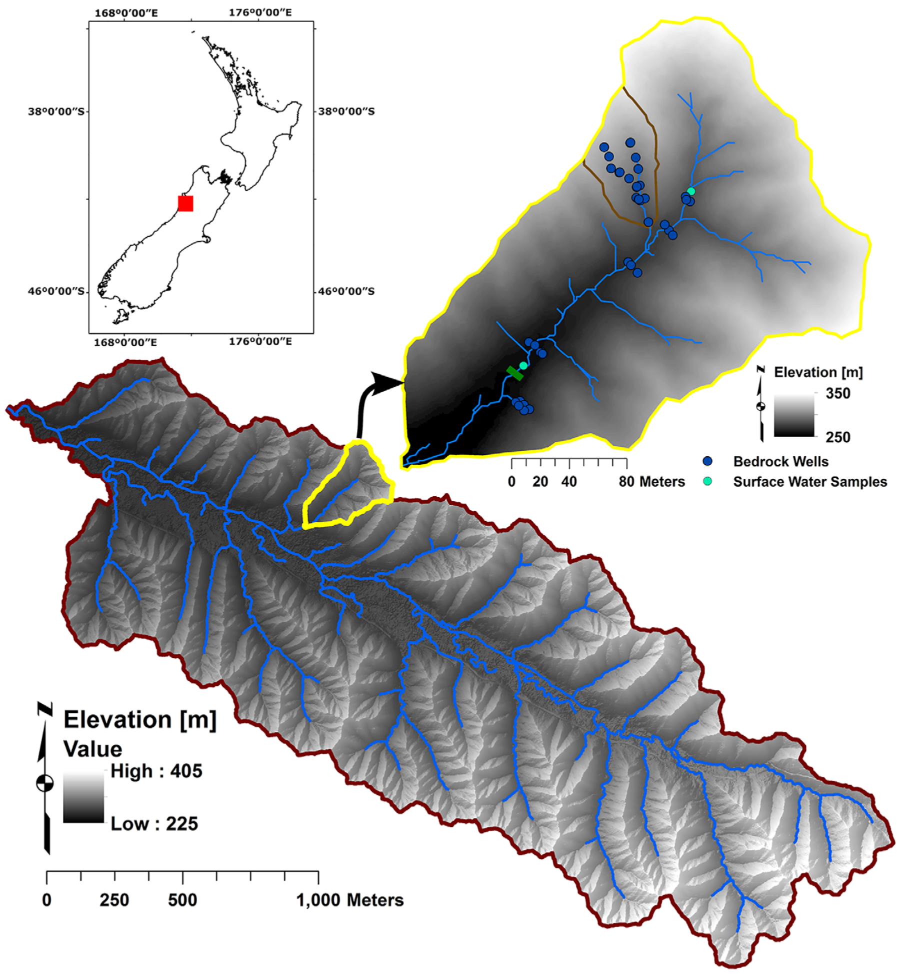

Figure 1. Map of the Maimai Experimental Watershed and subcatchment M8 with vicinity map inlay showing Maimai's general location within the country of New Zealand. The M8 subcatchment also shows the location of bedrock wells and the two surface water sampling locations. The green bar shows the location of the M8 weir and is the reference point for watershed area (4.5 ha).

formation known as the Old Man Group (Bowen, 1967). The gravel (now a weakly lithified conglomerate) was deposited in the early Pleistocene as a thick (>400 m) layer of glacial outwash during an erosional sequence in the formation of the Southern Alps (Mortimer et al., 2001). The conglomerate is composed primarily of rounded sandstone clasts (greywacke) with small additions of schist and granite in a compact sandy-clay matrix. The rounded clasts range in size from 10 to 400 mm in diameter, but are primarily less than 150 mm (Mortimer et al., 2001). Over the scale of a few meters, the bedrock is heterogeneous in clast size; however, over 10s–100s of meters the bedrock is relatively homogeneous (Nathan et al., 1986).

The entire M8 catchment, with the exception of the riparian zone (~5% of total area), was cleared of its native southern beech (*Fuscospora* spp.) and podocarp (*Podocarpaceae* spp.) forest in the 1970s and replanted with radiata pine (*pinus radiata*). The replanted forest was unmanaged and has proven susceptible to local fungal attack and windfall, leading to low stand densities and a thick undergrowth of invasive and native woody and herbaceous species. Rainfall interception losses for the original native vegetation, which is likely similar to the current vegetation cover, were measured by Pearce and Rowe (1979) and equal to ~670 mm/yr or ~ 26% of the 2,600 mm gross annual rainfall. Rainfall is spread over ~150 rain days/yr with a slight seasonality with drier conditions during midsummer months (January–March). Storms are generally characterized by their low-intensity and long duration. Mean rainfall intensity is 1.2 mm/h (Rowe & Pearce, 1994), although intensities >30 mm/h have been observed. Single event rainfall totals commonly exceed 100 mm. The catchment's low elevation and proximity to the Tasman Sea result in mild winters. Temperatures remain mostly above freezing, limiting snowfall occurrence to 1–2 days/yr with melt occurring within hours to days.

The thin soils, high frequency of storm events, and considerable precipitation maintain high soil water content throughout much of the year resulting in a highly responsive rainfall-runoff regime (Mosley, 1979). The Maimai has been described as the "quintessential steep humid catchment" (McGlynn et al., 2002, p. 3). Runoff ratios are among the highest of any research catchment in literature. Mean annual runoff is 1,550 mm, equal to nearly 60% of annual rainfall, and quick flow, as defined by Hewlett and Hibbert (1967), makes up >65% of annual runoff.

3. Data and Methods

3.1. Bedrock Characterization and Well Installation

Forty bedrock wells were drilled and completed within the M8 catchment for water table observation and groundwater extraction. Wells were strategically located in key landscape positions to capture the three main hydrologic response units (i.e., hillslopes, hollows, and riparian zones) that have been previously identified to be important for runoff generation at the Maimai (McGlynn & McDonnell, 2003b; Weiler et al., 2003). Fifteen wells were installed in hillslope positions, 14 in riparian and toe-slope positions, and 11 within the center of a previously studied ephemeral hollow (McDonnell, 1990; Mosley, 1979) (Figure 1). Except for Kosugi et al. (2011), we believe that this is the highest density of bedrock wells ever drilled in a small headwater research catchment.

Bedrock wells were installed using a modified version of the portable bedrock drilling system described by Gabrielli and McDonnell (2012). Bores were drilled to a diameter of 63 mm to varying depths depending on water table location (see Table 1 for details). PVC casing (25.4 mm inner diameter) was installed down the length of each bore and screened across the lower interval. Screened length was between 0.3 and 1.0 m, dependent on the completed depth into bedrock. We backfilled the well annulus with clean sand to a position 0.15 m above the top of the screened section and a bentonite slurry filled the remainder of the bore length to the soil surface. In locations where soil depth was greater than 0.15 m, a soil well was colocated with each bedrock well. Soil wells were completed to the depth of the soil-bedrock interface, screened across the lower 0.15–0.3 m dependent on soil depth, and backfilled in a manner similar to the bedrock bores.

Bedrock saturated hydraulic conductivity (Ksat) was determined in the field through falling head slug tests in each of the 40 bedrock bores. Slug tests were conducted by introducing a small volume of water instantaneously into the bore and monitoring the return of the water table to its initial depth. Slug test data were analyzed by implementing the Hvorslev method (Hvorslev, 1951) within the Aqtesolv software package. Tests were performed 1–3 times and in locations where more than one slug test was conducted the average value was calculated.

Table 1
Bedrock Well Characteristics Including Well Position Within the Landscape, Physical Well Characteristics, Associated Bedrock Characteristics, and Water Table Dynamics

Bedrock well	Landscape unit[a]	Total depth (m)	Depth into bedrock (m)	Screen length (m)	Distance to stream (m)	TWI	Mean Ksat ± 1 SD (m/s)	Mean landscape unit Ksat (m/s) (±SD)	Mean depth to water table (m)	Water table fluctuation range (m)	Water table sensitivity (mm/mm)	Spearman Rank	Transmissivity (m^2/s)
1	Hillslope	7.00	7.00		15.2	6.1	1.31E-08	$5.6E^{-08}$	6.89 ± 0.23	0.85	1.3 ± 2.3	0.65	1.8E-01
2	Hillslope	3.95	3.95		9.0	2.9	1.31E-08	($9.2E^{-08}$)	3.54 ± 0.11	0.52	1.4 ± 1.2	0.60	5.0E-04
3	Hillslope	7.14	7.14		12.3	3	6.9E-09						
4	Hillslope	1.51	1.51	0.5	5.8	2.2	2.48E-07 ± 2.25E-07		0.75 ± 0.16	0.81	4.7 ± 5.0	0.66	2.6E-02
5	Hillslope	4.46	4.46	1.0	5.6	2.2	1.60E-08 ± 7.62E-09		3.89 ± 0.16	0.85	3.9 ± 1.9	0.60	6.0E-04
6	Hillslope	3.86	3.16	0.5	14.5	3.6	7.18E-09 ± 3.52E-09						
7	Hillslope	6.33	5.67	1.0	14.4	3.6	2.77E-08 ± 1.65E-08						
8	Hillslope	6.49	5.69	1.0	26.8	5	1.50E-08 ± 4.56E-09		4.12 ± 0.11	0.45	1.6 ± 0.9	0.57	6.0E-04
9	Hillslope	5.57	4.15	1.0	35.3	4.6	2.97E-08 ± 1.43E-08		4.22 ± 0.14	0.71	2.0 ± 1.4	0.41	1.4E-03
10	Hillslope	8.80	7.49	1.0	35.1	4.6	6.26E-09 ± 3.22E-09		7.65 ± 0.09	0.36	1.0 ± 0.7	−0.30	2.0E-04
11	Hillslope	8.03	7.55	1.0	40.8	1.4	1.18E-08 ± 1.48E-09		6.19 ± 0.08	0.4	1.7 ± 1.3	0.20	4.0E-04
12	Hillslope	7.54	7.04	1.0	49.9	2.6	2.72E-07 ± 1.92E-07		6.84 ± 0.03	0.14	1.1 ± 0.8	0.71	5.1E-03
13	Hollow	1.49	0.94	0.3	0.8	9.1	4.00E-06 ± 1.97E-06	$6.8E^{-07}$	0.3 ± 0.18	0.91	6.0 ± 7.1	0.81	5.0E-01
14	Hollow	3.94	3.94	1.0	8.2	2.8	5.42E-09 ± 3.43E-09	($1.1E^{-06}$)	3.55 ± 0.03	1.12	4.5 ± 7.3	0.56	2.0E-04
15	Hollow	1.50	0.93	0.5	0.4	8.3	9.04E-08 ± 4.84E-08		0.52 ± 0.12	0.71	4.31 ± 5.1	0.76	9.7E-03
16	Hollow	1.42	0.82	0.5	1.4	5.5	1.38E-06 ± 6.91E-07		0.88 ± 0.08	0.42	3.6 ± 3.3	0.56	7.4E-02
17	Hollow	2.73	2.28	0.5	1.7	5.5	6.75E-07 ± 4.64E-07		1.67 ± 0.06	0.38	2.8 ± 2.5	0.71	3.5E-02
18	Hollow	2.81	2.15	0.5	4.2	3.4	4.42E-08 ± 1.77E-08		1.86 ± 0.14	0.78	2.6 ± 1.6	0.54	3.1E-03
19	Hollow	1.49	0.99	0.5	0.6	6.9	1.68E-08 ± 9.48E-10		1.15 ± 0.09	0.5	2.9 ± 5.3	0.25	1.1E-03
20	Hollow	1.80	1.68	0.5	1.4	7.9	5.81E-09 ± 6.41E-10		0.9 ± 0.09	0.52	1.4 ± 0.9	0.18	2.0E-04
21	Hollow	1.22	1.07	0.5	0.1	7.3	3.13E-08		0.47 ± 0.06	0.36	1.3 ± 1.2	0.85	1.3E-03
22	Hollow	2.25	1.36	0.5	14.3	3.7	7.65E-07						
23	Hollow	6.02	5.11	1.0	14.3	3.7	4.84E-07 ± 3.14E-07		4.55 ± 0.05	0.38	2.9 ± 1.9	0.86	2.9E-02
24	Riparian	4.01	2.27	1.0	9.8	4.3	3.50E-05	$1.3E\text{-}0^{5}$	1.57 ± 0.05	0.38	3.6 ± 2.5	0.69	2.9E+00
25	Riparian	2.79	0.81	0.3	8.7	5.1	1.09E-05 ± 5.22E-06	($1.7E^{-05}$)	1.33 ± 0.1	0.64	3.3 ± 2.0	0.95	1.1E+00
26	Riparian	1.90	0.95	0.3	0.6	13.2	2.59E-05 ± 2.27E-05		0.41 ± 0.13	0.83	6.3 ± 4.9	0.43	4.1E+00
27	Riparian	0.75	0.54	0.3	0.2	11.1	1.87E-05 ± 1.14E-05		0.26 ± 0.06	0.44	2.6 ± 2.7	0.87	1.3E+00
28	Riparian	2.05	1.63	0.5	3.3	3.7	6.98E-06 ± 2.29E-06		1.27 ± 0.09	0.65	4.2 ± 2.6	0.93	5.9E-01
29	Riparian	1.87	0.93	0.5	1.8	8.6	5.66E-06 ± 6.03E-07		0.55 ± 0.12	0.88	5.1 ± 5.5	0.46	8.1E-01
30	Riparian	4.00	3.62	1.0	4.6	5.6	1.93E-06 ± 2.08E-07		2.38 ± 0.15	0.9	6.2 ± 3.7	0.78	1.8E-01
31	Riparian	1.33	1.25	0.5	6.0	3.9	1.02E-06 ± 5.15E-07		0.98 ± 0.09	0.42	2.3 ± 1.4	0.92	6.3E-02
32	Riparian	1.69	1.35	0.5	1.2	7.4	7.01E-07 ± 1.46E-07		0.47 ± 0.05	0.31	3.1 ± 1.8	0.83	5.2E-02
33	Riparian	2.06	0.97	0.5	3.7	5.6	1.40E-06 ± 9.88E-07		1.06 ± 0.07	0.41	3.6 ± 2.6	0.65	6.1E-02
34	Riparian/Hill	5.60	5.60		6.5	7.1	6.99E-05		3.3 ± 0.06	0.26	1.5 ± 0.6	0.82	3.5E+00
35	Riparian/Hill	5.87	5.87		8.9	7.1	6.22E-06		5.68 ± 0.08	0.41	1.7 ± 1.3	0.74	1.5E+00
36	Riparian/Hill	3.34	3.34		5.0	5.4	2.38E-05		1.42 ± 0.04	0.16	1.6 ± 0.8	0.50	2.0E-04
37	Riparian/Hill	3.01	1.64	0.5	10.3	5.8	3.31E-06 ± 2.29E-06		2.05 ± 0.04	0.26	0.9 ± 0.6	0.61	8.8E-02
38	Riparian/Hill	3.36	1.44	0.5	7.5	5.2	2.48E-07 ± 2.75E-08		2.56 ± 0.22	1.13	6.0 ± 6.2	0.54	5.0E-02
39	Riparian/Hill	4.19	4.07	1.0	10.1	0.9	9.02E-06 ± 3.56E-06		3.34 ± 0.14	0.79	2.8 ± 2.6	0.63	4.2E-01
40	Riparian/Hill	5.08	3.85	1.0	7.1	3.2	4.98E-07 ± 1.18E-07		3.5 ± 0.23	1.36	4.0 ± 2.2	0.79	3.2E-02

Note. TWI refers to topographic wetness index (Beven & Kirkby, 1979). Spearman rank correlation coefficients are between storm event catchment discharge dynamics and water table dynamics for each well.

[a]Landscape positions classified as Riparian/Hill indicate wells located on hillslopes but drilled to a depth, where the screened interval was equal to or deeper than the ground surface of the local riparian zone.

Bedrock porosity was measured from large bedrock samples (~0.04 m^3) cut from the surface of the intact bedrock formation using a concrete cutting chainsaw (Stihl GS 461). Samples were transported to the University of Saskatchewan where porosity was determined using a water-displacement method. A sample was slowly saturated from the bottom up to reduce pore-space air entrapment and left submerged for 20 days. Saturated mass was measured and the sample was oven dried at 60°C until recursive weight measurements showed no additional mass loss, establishing the oven-dry mass. Mass difference between saturated and oven-dry states was divided by total sample volume to calculate porosity.

3.2. Bedrock Groundwater Dynamics and Flux

Streamflow, precipitation, soil, and bedrock water table position from 11 December 2014 to 31 January 2016, representing 416 days of monitoring. Streamflow was measured at the M8 catchment outlet at 10 min intervals using a 90° V-notch weir. Stage height was converted into specific discharge using a standard rating curve for 90° sharp crested V-notch weirs (Rantz, 1982). Rainfall was recorded using a 0.2 mm tipping bucket rain gauge located within the M8 catchment 20 m downstream of the main weir (Figure 1).

Soil and bedrock wells were instrumented with absolute pressure transducers (OnSet Loggers© or Heron Instrument©) or capacitance rods (Tru-Track© or Odyssey Instruments©) to record water table location and dynamics in each well at 10 min intervals. Two pressure transducers were located within a research hut 100 m from the M8 outlet to record barometric pressure in order to correct absolute pressure readings from the deployed pressure transducers. Tru-Track© and Odyssey© capacitance rods had a blanking distance of 75 and 35 mm, respectively, which prevented the observation of saturated conditions below these lower ranges for soil and bedrock wells instrumented with this equipment.

We used basic metrics to quantify the spatial and temporal patterns of event-based and seasonal water table fluctuations for each bedrock well, and identified average values for wells clustered within similar landscape units. We calculated storm response, defined as millimeters of water table displacement per millimeter of rainfall for each storm event. We also calculated a storm transmissivity change metric, equal to the change in water table depth multiplied by local bedrock hydraulic conductivity, where the change in depth was defined as the difference in water table elevation between prestorm and storm-peak levels. This value allows for a more consistent comparison of water table dynamics between wells in different landscape units by accounting for the effect of spatially varying hydraulic conductivity. Higher values of transmissivity change are associated with greater groundwater flux. Additionally, Spearman rank correlation coefficient (ρ), a nonparametric measure of statistical dependence between two variables, was used to test the relationship between water table fluctuations and catchment discharge.

We calculated vertical hydraulic gradient between 17 colocated soil and bedrock wells and 3 colocated bedrock wells and used this data set to establish spatial and temporal trends of vertical bedrock groundwater gradients across the catchment and to map the general flow structure within the groundwater flow domain. Gradients were categorized as either vertically upward, vertically downward, or hydrostatic. We considered the hydraulic gradient to be hydrostatic when differences in potentiometric surfaces were within 20 mm.

3.3. Transit Time Estimation

Tritium (^3H)-based MTT and mean groundwater age estimates were conducted on water samples collected during a synoptic sampling campaign during a low-flow period on 24 February 2015. Two surface water, 3 soil water, and 23 bedrock groundwater samples were taken from locations within M8. To remain consistent with literature, we report stream sample ages as MTT and soil and bedrock samples as groundwater age. Although it is recognized that measurements of mean transit time or mean groundwater age carry limited information in comparison to full transit time distributions (McDonnell et al., 2010), MTT still provides fundamental understanding of catchment storage-release trends and allows for beneficial comparisons between catchments across hydroclimatic and geologic spectra.

Additionally, while much theoretical progress is being made in transit time distribution modeling (Berghuijs & Kirchner, 2017; Harman, 2015; Rinaldo et al., 2015) field limitations continue to constrain efforts to fully characterize whole-catchment flow path distributions. We determined stream water MTT and groundwater age estimates by employing a lumped parameter convolution approach as outlined in Małoszewski and Zuber (1982):

$$C_{out}(t)=\int_0^\infty g(\tau)C_{in}(t-\tau)e^{-\lambda\tau}d\tau \quad (1)$$

where $C_{out}(t)$ is the ^3H concentration of individual samples at time t, $g(\tau)$ is the transit time distribution, C_{in} is the ^3H concentration of precipitation into the system, and $e^{-\lambda\tau}$ is the radioactive decay term to account for the natural decay of the tritium isotope, where the decay constant $\lambda=\ln\left(2/T_{1/2}\right)$ and $T_{1/2}=12.32$ years for ^3H.

C_{in} was determined from long-term monthly tritium measurements made at the Kaitoke reference station near Wellington, New Zealand, approximately 150 km north of Maimai. We scaled rainfall input at Maimai by a factor of 1.15 based on a standard latitude adjustment and verified this scaling factor with tritium measurements taken from two aggregated rainfall samples collected over a 10 month period at the outlet and upper elevations of the larger Maimai watershed that M8 is located within. See supporting information Figure S2 for the tritium input function at Maimai.

Tritium concentrations, used to define C_{out}, were analyzed by the GNS Science Water Dating Laboratory (Lower Hutt, New Zealand) using electrolytic enrichment and liquid scintillation counting (Morgenstern & Taylor, 2009). Recent advancements in this method have led to further tritium enrichment that is now >90-fold, leading to a lower detection limit of 0.02 tritium units (TU). The decay of tritium from hydrogen bomb testing in the 1960s and 1970s to very low levels in New Zealand results in MTT estimates that are relatively insensitive to the model choice (i.e., g(τ)) when estimating the transit time distribution of the studied flow system—meaning the shape of the model (i.e., the *f*-value) is no longer critical for accurate and unambiguous MTT estimates (Morgenstern et al., 2010). We used a uniform exponential piston flow model with 70% exponential flow within the total flow volume—which was found to be a reasonable ratio by Morgenstern et al. (2010)—to estimate $g(t)$ as follows (Małoszewski & Zuber, 1982):

$$g(\tau)=0 \text{ for } \tau<\tau_m(1-f) \quad (2)$$

$$g(\tau)=(f\tau_m)^{-1}\exp\left[-\left(\frac{\tau}{f\tau_m}\right)+\left(\frac{1}{f}\right)-1\right] \text{ for } \tau\geq\tau_m(1-f) \quad (3)$$

where f represents the ratio of the exponential flow volume to total flow volume and τ_m is the mean age in years. To highlight the relative insensitivity of mean age estimates to the selected *f*-values within the model, we conducted a sensitivity analysis by varying *f* from 40% to 100%. We also compared age results from the dispersion and gamma models with the exponential piston flow model following Stewart et al. (2017). We focus on results for the exponential piston flow model with *f* equal to 70%; however, results for the sensitivity analysis and comparison to dispersion and gamma models can be found in supporting information.

3.4. Silica Analysis and Catchment Transit Time

To estimate a series of stream water transit times for catchment M8 discharge, we followed an approach similar to Peters et al. (2014). An empirically derived relationship between groundwater silica concentration, tritium-based groundwater age, and stream water silica concentrations was used to estimate stream water TT. Dissolution from water-rock interactions tends to increase groundwater silica concentrations with increased subsurface contact time allowing silica to be used as a proxy for stream TT (Burns et al., 2003; Edmunds & Smedley, 2000; Katz et al., 2004; Stewart et al., 2007). We established two regression relationships; one between catchment discharge volume and catchment discharge-silica concentration, and a second between silica concentration in soil and bedrock water samples and tritium-based age measured at those sampling locations. The discharge-silica relationship was developed from grab samples collected during a moderate sized storm event (35 mm rainfall) from the M8 catchment outlet at intervals which captured pre-event, event and recession conditions. Thirteen water samples were collected in 250 mL HDPE bottles, filtered using 0.45 μm cellulose acetate syringe filters, and refrigerated within 24 h of sampling. Analysis was conducted at the Oregon State University Collaboratory using an ion chromatograph (Dionex ICS-1500). We applied the discharge-silica regression model to the time series of catchment runoff to produce an estimated stream water silica concentration at 10 min intervals for 1 year (25 December 2015 to 24 December 2016). We then applied the silica-groundwater age regression model to the silica time series to estimate stream water TT over the same period. This produced a 1 year time series of estimated stream water TT covering more than 60 storms and seasonal shifts in catchment wetness conditions and water balance.

10.1029/2017WR021825

4. Results

4.1. Bedrock Characterization

Lab-based porosity measurements of bedrock samples taken from the upper 1 m of bedrock had an average value of 0.21 (n = 3, standard deviation = 0.03), which is within the range of established porosities for sandstone (Freeze & Cherry, 1979).

Variability in Ksat for all bedrock wells spanned 5 orders of magnitude and ranged from 5.42E-9 to 6.99E-5 m/s (Table 1). Slug tests revealed spatial patterns in Ksat that broadly followed geomorphic landscape units. Mean Ksat increased from hillslopes to hollows to the riparian zone with mean values each of 5.6E-08, 6.8E-07, and 1.3E-05 m/s, respectively. Mean Ksat between hillslope and hollow values was not statistically significant (P-value 0.068), but was statistically significant between hillslope and riparian and hollow and riparian (P-value 0.015 and 0.033, respectively). The increase in conductivity with increasing upslope accumulated area may indicate that wetter zones with greater upslope area undergo greater mineral weathering resulting in more permeable bedrock.

4.2. Bedrock Groundwater Position

Bedrock groundwater was present in the majority of wells over the entire study period (Table 1); however, during an unusually dry period between December 2014 and February 2015, water tables dropped below well screens in some riparian and ephemeral hollow locations. We note that January 2015 was the single driest month in 660 months of record at the Reefton meteorological station 5 km southeast of Maimai.

Water table depths ranged from 0.26 to 7.65 m below the ground surface. Generally, the water table was shallower in the riparian zone and at the center of the hillslope hollows and deeper in toe-slope and upper hillslope positions (Table 1). We fit a relation between depth to water table and distance to stream channel with a power-law regression ($R^2 = 0.72$) and applied this to a 1 m grid DEM of M8 to produce a catchment scale water table map (Figure 2). Figure 2 shows the shallow water table in topographically convergent areas and a rapid deepening of the water table with distance from the stream channel. Estimated depth to water table ranged from 0.98 m in the near-stream riparian corridor to approximately 10.5 m at ridgeline. Mean, median, and standard deviation of depth to water table over the entire catchment domain were 5.25, 5.43, and 2.03 m, respectively.

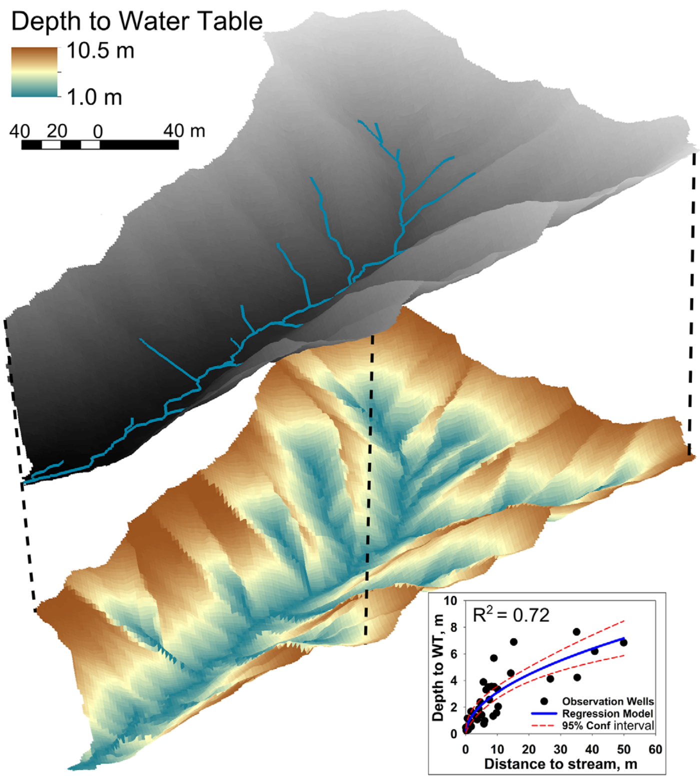

Figure 2. Depth to water table for the underlying headwater bedrock aquifer based on average water table depths over 400 days from 36 monitored bedrock wells. Depth to water table is overlaid on the three-dimensional representation of the bedrock aquifer free-water surface. The M8 three-dimensional DEM is included above the water table layer for visual comparison. The inset scatter plot shows the relationship between distance to stream and depth to water table ($R^2 = 0.72$).

4.3. Bedrock Groundwater Dynamics

A representative example of water table dynamics for each of the three main landscape positions is shown in Figure 3. Although there was variability within each landscape position, event-based water table fluctuations, seasonal fluctuations, storm response, and transmissivity change metrics all captured consistent trends delineating the three landscape units. Generally, lower-lying areas had a greater range and variability, while dynamics became more attenuated with distance from the stream channel.

Seasonally, maximum water table fluctuation for all wells over the monitoring period ranged from 0.14 to 1.36 m. The range in seasonal water table fluctuations was greatest in the shallower riparian and toe-slope zones. Seasonal fluctuations were smaller in wells located in the center of hollows and even smaller further in the upper hillslope positions (i.e., wells 8, 9, 11, 12). Upper hillslope wells displayed almost no seasonal fluctuations, with the most near-ridge well (well 12) fluctuating only 0.14 m cm during the study period, which included one of the driest periods on record.

Average event-based water table response (measured as mm change in water table per mm of rainfall) for each well over the 70 monitored storm events is presented in Table 1. Spatially averaged response was

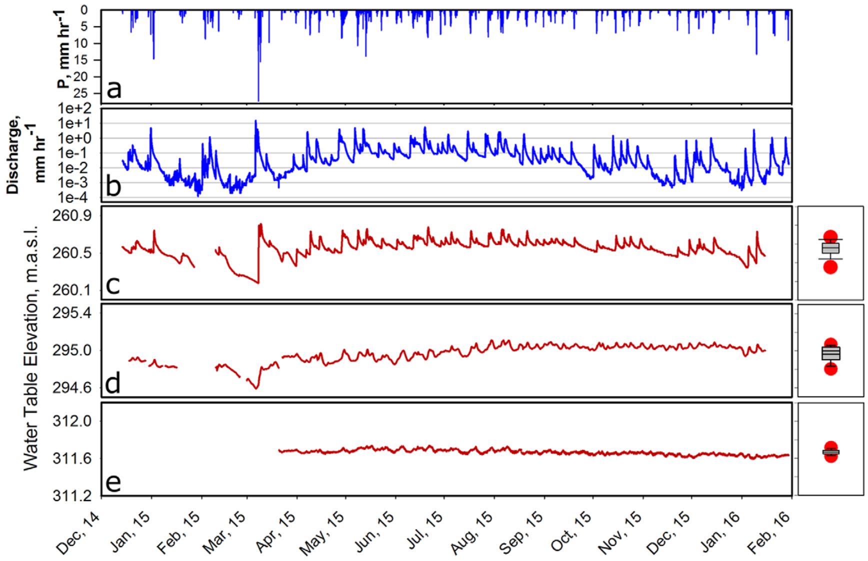

Figure 3. (a) Rainfall, (b) runoff time series along with water table elevation data from a representative (c) riparian, (d) hollow, and (e) hillslope wells. Box and whisker plots show median, and first and third quartiles of the water table dynamics for each of the three landscape positions.

Table 2
Tritium Units and Corresponding Groundwater Age and MTT for Bedrock, Soil, and Stream Water Samples Within the M8 Catchment, Respectively

Well/sample name	Landscape position	Tritium units (TU)	±1 SD (TU)	Groundwater age/MTT (years)
8	Hillslope	1.38	0.03	10.5
12	Hillslope	1.65	0.04	6.5
13	Hollow	2.11	0.04	0.3
16	Hollow	2.14	0.04	0.3
17	Hollow	2.01	0.04	0.3
21	Hollow	1.87	0.04	1.3
23	Hollow	1.73	0.03	5.3
24	Riparian	1.24	0.03	13.5
25	Riparian	1.85	0.03	2.5
26	Riparian	1.98	0.03	0.7
27	Riparian	2.10	0.04	0.3
28	Riparian	2.17	0.04	0.3
29	Riparian	2.05	0.04	0.3
30	Riparian	2.06	0.03	0.3
32	Riparian	2.13	0.04	0.3
33	Riparian	2.18	0.05	0.3
34	Riparian/Hill	0.97	0.02	23
35	Riparian/Hill	1.01	0.03	22
36	Riparian/Hill	1.02	0.02	22
37	Riparian/Hill	1.72	0.03	5.5
38	Riparian/Hill	2.16	0.04	0.3
39	Riparian/Hill	1.72	0.03	5.3
40	Riparian/Hill	2.17	0.04	0.3
41	Soil-Riparian/Hill	2.05	0.04	0.5
42	Soil-Riparian	2.15	0.04	0.3
43	Soil-Hollow	2.50	0.05	0.1
44	Stream-Upper Riparian	1.85	0.03	0.3
45	Stream-Weir	2.11	0.04	2.5

Note. Samples 41, 42, and 43 are soil wells, sample 44 is a stream sample from the same catchment location as soil well 42, and sample 45 is from the main M8 weir.

3.9, 3.23, and 1.96 mm/mm for riparian, hollow, and hillslope locations, respectively. Water table response and transmissivity change captured similar spatial trends to those observed for average event-based and seasonal water table fluctuations, generally indicating greater damping with distance from the stream channel (Table 1). The mean hillslope, hollow, and riparian bedrock transmissivities each increased progressively by an order of magnitude, from 3.76×10^{-8} to 4.79×10^{-7} to 5.35×10^{-6} m^2 s^{-1}, respectively.

Spearman rank correlation coefficients between catchment discharge and water table dynamics decreased from the riparian zone to hollow to hillslope (Table 1). Riparian zone wells were extremely responsive to precipitation inputs with rapid water table rises and recessions in phase with the storm hydrograph ($\rho = 0.71$). Ephemeral hollow wells responded to individual storm events but were slightly more delayed and attenuated than the riparian zone ($\rho = 0.61$), while hillslope wells had an even more attenuated storm response; water table rise and fall was not always attributable to specific storm events ($\rho = 0.52$) (Figure 3).

4.4. Bedrock Groundwater Gradients

Groundwater head gradients across the catchment were predominantly downward in all landscape positions (Figure 4) indicating that the catchment is continuously recharging surface and soil water into the bedrock groundwater aquifer. Hillslope head gradient calculations were sporadic based on the transient nature of saturated hillslope soils which occurred only during wet antecedent moisture conditions or during larger storm events. Within the ephemeral hollow, soil-bedrock well pairs showed consistent downward head gradients across all wetness conditions and storm intensities, with the exception of the most downslope well pair (well 13 and associated soil well). Transient flow reversals occurred during storm event peaks under wet

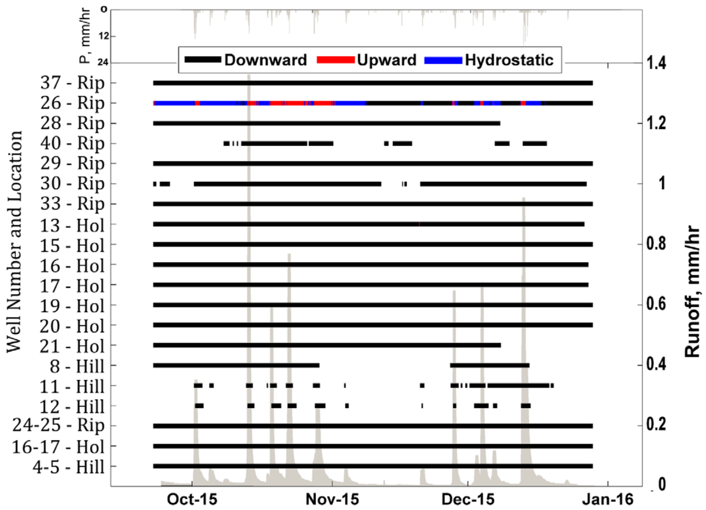

Figure 4. Vertical groundwater head gradients between nested soil-bedrock wells (shown by a single well number on the *y* axis) and nested bedrock-bedrock wells (shown as two well numbers on the *y* axis). Colored horizontal bars represent gradient direction. The white space within horizontal bars is indicative of dry periods when no soil water was present in the wells, thus no gradient was calculated. The exception to this is the late periods wells 28 and 21 which were missing data due to instrument failure. Additionally, rainfall and runoff data are displayed for the corresponding time period. Note, data logger failure prevents full display of time series—however, trends in the overall data do not deviate significantly from the subset presented.

antecedent moisture conditions, resulting in hydrostatic conditions, or upward soil well gradients at the base of the hollow.

The riparian corridor groundwater flux was also consistently downward. The exception to this trend was the most downstream well pair (well 26 and associated soil well) located 15 m upstream from the M8 weir. During wet conditions, the hydraulic gradient remained hydrostatic between storm events and briefly switched upward during rainfall periods. During drier conditions gradients also switched to upward (or hydrostatic) during rainfall events, but remained downward between events. Under extremely dry conditions (not shown in Figure 4) upward gradients prevailed, indicating bedrock groundwater subsidies to base flow (as discussed below). For this well pair (well 26), hydraulic gradients were upward, hydrostatic, and downward for 27%, 26%, and 47% of the monitoring period.

4.5. Tritium Measurements Groundwater Age and Stream Water MTT

A synoptic sampling of 30 locations on 24 February 2015 within the M8 catchment produced tritium-based age estimates for 2 surface water samples, 3 soil water samples, and 23 bedrock groundwater samples. The catchment was extremely dry, with a 30 day antecedent precipitation index (API) value of 25.2 mm (API as defined by Kohler and Linsley (1951)), and a catchment discharge of 0.00075 mm/h corresponding to a flow exceedance probability of 99%. Table 2 presents tritium concentrations and estimated MTT for each sampling location. We tested various model shapes (i.e., *f*-values) for both surface and groundwater samples and the resulting estimated ages are provided in supporting information Table S1. No significant difference was noted in sample ages using the various *f*-values, so we focus on results for age values reported for an *f*-value of 70%. Groundwater age for all bedrock wells ranged from less than 0.1 to 23 years (>2.50 to 0.97 TU, respectively). The three soil water samples taken from hillslope, toe-slope, and riparian positions had ages less than 0.5 years. Soil water sample 43, collected from a perennial soil seep within the instrumented hollow, was the youngest of all waters tested with a value of >2.50 TU. This is similar in concentration to recent precipitation, indicating extremely short travel times. Sample 42 from the most upstream portion of the riparian zone had a value of 2.15 TU, corresponding to an age of 0.3 years, which is identical to the surface water collected in the same location (sample 44). Soil water sample 41, collected from a perennially saturated soil well at the base of a short planer hillslope near the catchment outlet, had a tritium concentration of 2.05 TU, corresponding to a groundwater age of 0.5 years.

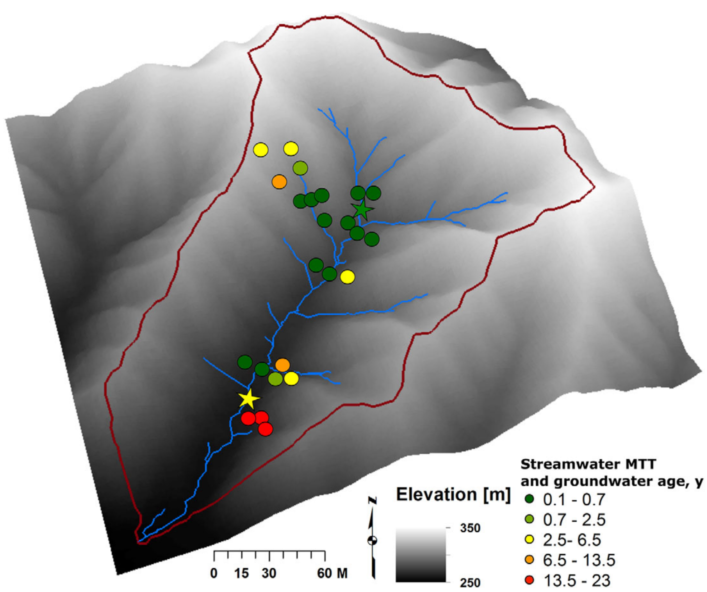

Figure 5. Spatial distribution of soil and bedrock groundwater age and stream water MTT across the M8 catchment. Bedrock and soil samples are indicated by colored circles and surface samples are indicated by stars.

Bedrock groundwater within M8 ranged in tritium concentration from 2.18 to 0.97 TU (groundwater age 0.3–23 years, respectively) indicating that the water in the underlying aquifer includes a wide range of ages representing heterogeneous flow paths (Figure 5). The bedrock groundwater age varied both spatially and with depth, revealing complex spatial patterns associated with the groundwater flow structure. Groundwater age was weakly related with well depth ($R^2 = 0.32$). All groundwater samples older than 2.5 years were found at depths greater than 2.8 m, while the youngest waters were found predominantly in shallower wells. There was no significant correlation between groundwater age and depth to water table, upslope accumulated area, or the topographic wetness index (as calculated by Beven and Kirkby (1979)).

Generally, upper hillslope and deep riparian and toe-slope positions contained the oldest water, while younger water was found primarily in shallow bedrock wells within hollow and riparian positions. Bedrock wells along the entire length of the ephemeral hollow generally had younger water. All groundwater age estimates for wells within the hollow were less than 1.3 year old (>1.87 TU), with the exception of the most upslope well, well 23, which had an age of 5.3 years (1.73 TU). The location, depth to water table and water table dynamics of well 23 were more characteristic of other hillslope wells, as opposed to hollow wells, and as such, the older groundwater at this location was expected. The two upper hillslope samples (wells 8 and 12), collected at depths greater than 7 m, had groundwater ages of 6.5 and 10.5 years, respectively (1.65 and 1.38 TU, respectively).

Riparian zone and toe-slope wells had the greatest water age and ranged from 0.1 to 23 years (2.5 and 0.97 TU). All toe-slope and riparian wells in the upper portion of the catchment, regardless of exact landscape position, contained young waters less than 0.3 years (TU > 2.01). Further downstream in the riparian zone, shallow wells remained young while deeper wells contained older water (>5 years, TU < 1.72). The oldest waters were found in toe-slope positions on the east side of the catchment within 20 m upstream and downstream of the catchment outlet. These wells (24, 34, 36, 37, and 39), all with sampling depths greater than 3.0 m, had estimated ages of 23, 22, 5.5, 13.5, and 5.3 years, respectively.

4.6. Silica and Time-Varying Stream Water TT

The regression model captured the strong linear relation between the log-transformed values of discharge and silica ($R^2 = 0.98$; Figure 6a). Silica concentration showed strong dilution with increasing discharge. When applying this relationship to 1 year of catchment runoff, the estimated catchment discharge-silica concentration dropped to a low of 3.14 mg/L during peak storm events and rose to a high of 19.4 mg/L during an extended dry period in early 2015 (Figure 7b).

Using the relation between the derived silica concentration and groundwater age (Figure 6b, $R^2 = 0.92$) we estimated stream water TT from the 1 year time series of silica concentration (Figure 7c). TT ranged from 0.37 to 2.5 years. Time-weighted mean TT was 0.62 years and the volume-weighted mean was 0.41 years. The TT time series showed a distinct bimodal age distribution that followed seasonal catchment wetness conditions and discharge volume. During the drier months of December through February, the catchment was in a state of older low-flow discharge punctuated by occasional precipitation inputs that transiently flushed young water to the stream channel. Base flow conditions quickly reestablished post storm-hydrograph peaks and TT increased. Beginning in March, precipitation became more persistent, the growing season slowed and temperatures declined, reducing the evapotranspiration budget. Base flow discharge increased between events as the catchment wetted up, available storage declined and the streamflow became younger. Catchment wet-up continued through April until soil water storage filled and antecedent wetness remained high between events, indicated by sustained high runoff. This tipped the catchment into a state of young water discharge and stream water TT remained short and relatively stable

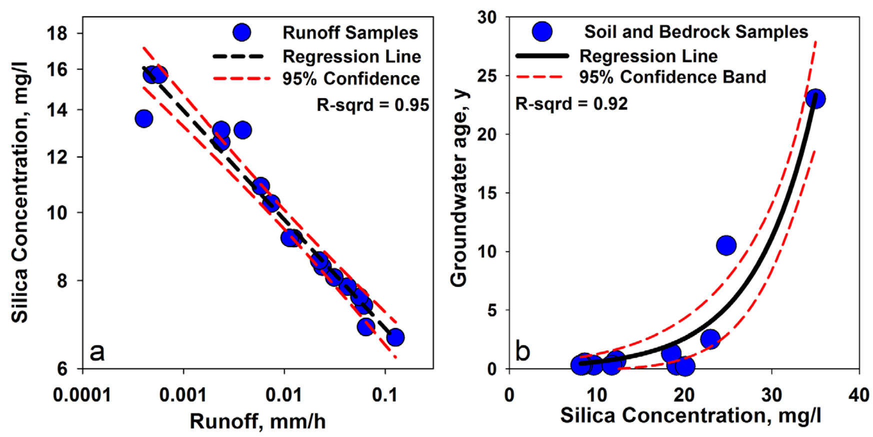

Figure 6. (a) Linear relationship between the log-transformed M8 stream specific discharge and stream water silica concentration and (b) nonlinear relationship between silica concentration in bedrock groundwater and soil water and measured groundwater age. Both plots show values for individual grab samples, the fitted regression model, and 95% confidence interval.

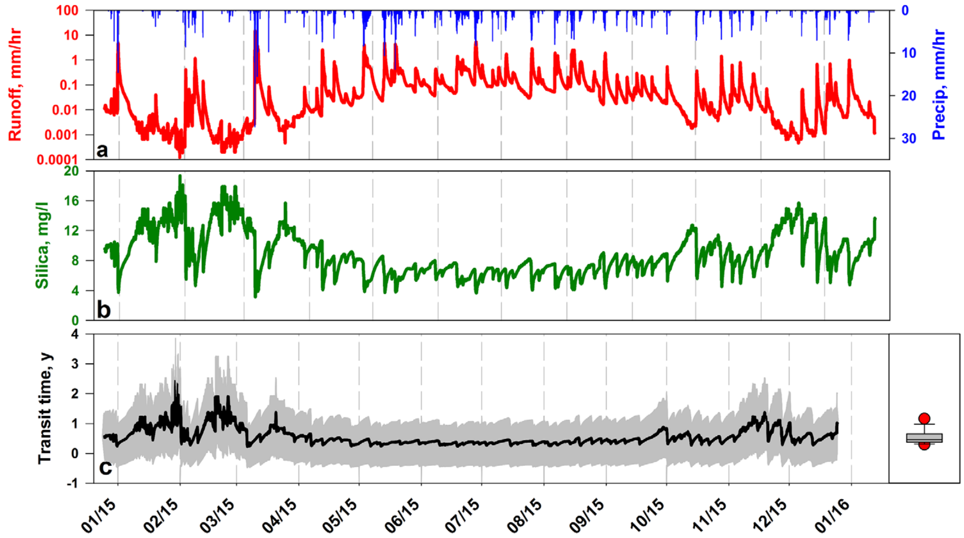

Figure 7. (a) Time series of precipitation and runoff, (b) estimated stream water silica concentration and (c) estimated stream water TT with 95% confidence band. The blue hashed line represents the time-weighted stream water TT (0.62 years) and the red hashed line represents the volume-weighted stream water TT (0.41 years). The box plot shows median, first, and third quartiles. Whiskers are equal to the 10th and 90th percentiles and red dots are outliers at the 5th and 95th percentiles.

through the remainder of the wet season. Beginning in October/November the catchment began to dry up as the next growing season initiated. As a result, stream water TT became much more dynamic and again fluctuated between low-flow older and event-driven younger periods.

5. Discussion

Our intensive process-based hydrometric, hydrochemical, and isotopic field campaign focused directly on characterizing the location, dynamics, and age of the bedrock aquifer and its contributions to streamflow. We found contrasting groundwater and streamflow ages at the Maimai watershed—supporting the recent quantitative theoretical work of Berghuijs and Kirchner (2017). The volumetric contributions of old bedrock groundwater to runoff generation were limited by low bedrock permeability. Catchment storage was dominated by contrasting domains of shallow, young soil water versus deep and much older bedrock water and aquifer storage. Young soil contributions to streamflow masked bedrock groundwater influence on stream water transit time except for short dry periods during summer base flow conditions.

5.1. What Controlled Bedrock Groundwater Location and Dynamics?

5.1.1. Water Table Position

We found that the shape of the underlying bedrock aquifer reflected a subdued replica of the land surface (Figure 2). This is consistent with other field and modeling studies in humid regions and suggests a topographically controlled water table (Haitjema & Mitchell-Bruker, 2005; Sanford, 2002; Winter et al., 2003). While the topographic control on water table position is not surprising given early descriptions of this (Todd, 1956), what was surprising was the particularly shallow ridgeline water table positions in the M8 catchment. This is in stark contrast to catchments in other geologic settings with similar climatic regimes (Hale et al., 2016; Haria & Shand, 2004; Katsura et al., 2008) and especially other watersheds where we have worked—e.g., WS 10 at the HJ Andrews Watershed, where ridgeline water tables were very deep and fluctuated greatly between the dry and wet seasons (Harr, 1977). The depth to ridgeline water table exemplifies the complex interrelationship between climate, topography, and geology, representing the balance point between recharge inputs from above and the ability of the bedrock formation to transmit water downgradient (Jamieson & Freeze, 1982). In a simple sense, the Maimai's shallow ridgeline water tables represent reduced groundwater flux compared to other sites with deeper water tables under similar recharge and geologic conditions (Fetter, 2000). The lower hydraulic conductivity limits the flux, forcing the water table to rise, increasing the hydraulic gradient until bedrock groundwater recharge is balanced with discharge. As a metric, ridgeline water table depth, when considered along with the local precipitation regime, can provide insight on the landscape scale hydrologic importance of bedrock in terms of the extent of water movement. This also provides some understanding into the relative amounts of active storage and total catchment storage and their links to flow and transport. For example, a high water table in a hydrologically responsive catchment would imply a smaller vertical groundwater flux and greater horizontal partitioning of precipitation inputs to shallower flow paths, thus greater volumes of younger water contributing to runoff. Conversely, a high ridgeline water table in a catchment with a dampened stream response would indicate greater vertical recharge to depth, larger active groundwater storage and greater volumes of older water contributing to runoff (Tague & Grant, 2004).

Gleeson and Manning (2008) used 3-D numerical simulations to explore the control of recharge rates and hydraulic conductivity on water table location. They found that increasing the ratio of recharge (R) to hydraulic conductivity (K) resulted in higher water table elevations. Indeed, the R/K ratio at Maimai is 0.64 (recharge 200 mm/yr and bedrock hydraulic conductivity of 1.0×10^{-8} m/s), equal to the highest R/K value explored by Gleeson and Manning (2008). The high R/K ratio that we observed at M8 is consistent with the Gleeson and Manning (2008) prediction of the shallow ridgeline water table at our site.

5.1.2. Water Table Dynamics

Groundwater dynamics at M8 were spatially and temporally variable with some distinctions between the three major landscape units (Figure 3). The spatially variable water table dynamics revealed locally complex interactions between topography, aquifer characteristics, recharge source and timing, as well as pressure propagation through the vadose zone.

Seasonally, water table dynamics were most variable in the riparian zone and hollow positions and least variable in near-ridge wells. This trend was opposite to what we expected. During drier summer months as the landscape drained, we expected that hillslope water table positions would drop significantly and the riparian water table position would remain relatively constant, as has been reported in hillslope studies in other humid catchments (Hale et al., 2016; Iwagami et al., 2010; Katsuyama et al., 2005; Kosugi et al., 2011, 2006). The absence of this trend at Maimai, where the near-ridge water table levels showed little seasonality, is likely due to the low hydraulic conductivity of the OMG formation, with its low hydraulic conductivity. The scarcity of bedrock fracturing at M8 forces recharge to occur through the bedrock's primary porosity, instead of through preferential fracture-based recharge, a flow process that has been previously attributed to large and rapid water table fluctuations (Gabrielli et al., 2012; Gleeson et al., 2009; Montgomery et al., 1997; Praamsma et al., 2009). Additionally, unsaturated bedrock storage increased with distance to the ridge as the vadose zone overlying the aquifer thickened. This low permeability unsaturated wedge likely smooths and buffers seasonal variations of bedrock infiltration, while also delivering a relatively constant rate of recharge to the free-water surface. These factors combined maintained the observed near-stationary hillslope water table position near the ridgeline.

In lower lying wetter zones where bedrock water tables were shallow, more pronounced dynamics were observed in response to storms and seasonally. The thin or nonexistent unsaturated zone in the bedrock in this area is not able to buffer the groundwater table from storm event inputs. The observed increased hydraulic conductivity in the riparian zone and ephemeral hollows (possibly a weathering feedback) caused a more pronounced decline in water tables during dry periods. This drove a spatially variable heterogeneous but structured groundwater drainage pattern that was correlated to wetter convergent regions of the catchment with greater groundwater mobility.

5.2. The Bedrock Groundwater Domain: Gradients, Age, and Flow Contributions to the Stream

Identifying the groundwater flow domain within small headwater catchments is often complex due to bedrock heterogeneity and considerable topographic relief that drives small-scale spatially variable flow paths (Fujimoto et al., 2014; Katsura et al., 2014; Kosugi et al., 2011; Masaoka et al., 2016; Oshun et al., 2016; Salve et al., 2012). Previous catchment studies have shown the value of combined hydrometric and tracer analyses to constrain runoff processes and develop conceptual hydrologic models that are both parsimonious and consistent with multiple data sets (Clark et al., 2011). Our extensive soil and bedrock well network provided the ability to independently identify the groundwater flow domain through hydrometric analysis (i.e., groundwater flow gradients (Figure 4)) and tritium-based MTT via groundwater isochrones (Table 2). The two data sets identified spatially consistent groundwater recharge and discharge zones within the catchment confirming contributions of bedrock groundwater to catchment runoff.

5.2.1. Bedrock Groundwater Gradients

Groundwater head gradients across all hillslope positions were downward and indicated no bedrock groundwater discharge along the catchment hillslopes, consistent with previous studies at M8 (Gabrielli et al., 2012) and many hillslope bedrock groundwater observations elsewhere (Katsura et al., 2014; Kosugi et al., 2011; Salve et al., 2012). Interestingly, downward groundwater gradients within most of the wetted riparian corridor, including the ephemeral hollow, indicated that for the majority of the observed study period the stream channel acted as a groundwater recharge source (as opposed to sink) for bedrock groundwater. Although losing streams are common across many landscapes (Sophocleous, 2002), they are much less common in humid headwater regions, where the riparian corridor is generally viewed as the discharge zone for deeper hillslope flow paths (Voltz et al., 2013). This presents new implications for land use management at M8 and other similar riparian recharged headwater catchments, because hillslope or shallow riparian-derived contaminants may be transported to depth more easily in these locations.

Upward groundwater gradients were observed at the base of the ephemeral hollow during the peak of storm events with wet antecedent conditions. The specific discharge calculated using the measured bedrock aquifer hydraulic conductivity and the well head gradient was a mere 0.5 L/h/m^2. Even assuming uniform discharge across the entire riparian corridor ($\sim$5% of catchment area), bedrock groundwater contributions to catchment runoff of this rate would only deliver 0.00025 mm/h (assuming direct connection to the stream channel), a rate too small to be measured or appreciably shift hydrometric or hydrochemical characteristics during event runoff periods.

Similar event-based discharge gradients were also noted at the most downstream riparian transect, but likewise were too small to measurably influence storm runoff characteristics. However, discharging bedrock groundwater at this location was found to appreciably contribute to catchment discharge under extremely low base flow conditions in the absence of recent rainfall input to the stream channel.

5.2.2. Bedrock Groundwater Age

Recharge and discharge zones represent the initiation and endpoints of groundwater flowlines (Salvucci & Entekhabi, 1995) thus, spatial patterns of groundwater age should mirror spatial patterns of the groundwater flow domain. Indeed, we found younger waters in recharge zones and correspondingly older water in discharge zones. Bedrock groundwater samples extracted from the recharging upper riparian corridor were among the youngest waters in the catchment, indicative of recent recharge from young overlying stream and soil water. In the lower riparian zone, older bedrock groundwater was colocated with discharging gradients suggesting stream water should reflect contributions from these older sources. Indeed, we found stream water to be 2.5 years, increasing in age from a computed 0.3 years only 120 m upstream. The independent agreement of groundwater head gradients with spatial groundwater age patterns not only provides direct source-area evidence of bedrock groundwater contribution to streamflow, but better informs process understanding of the catchment groundwater flow domain and surface water-groundwater interactions.

The lack of correlation between groundwater age and spatial and depth metrics is likely a result of the inability of one-dimensional or two-dimensional landscape-derived metrics to fully capture the complex three-dimensional groundwater flow structure and storage volume that sets groundwater age. This inability for simple topographic parameters to capture the groundwater age at Maimai may hint at why many other studies have also failed to find simple landscape-derived scaling metrics that accurately capture stream water MTT (Tetzlaff et al., 2009). In humid catchments, storage volume is critical in setting the age of discharge, and the degree to which any metric acts as a proxy for this storage volume likely controls the strength of its correlation to catchment MTT (McNamara et al., 2011). In steep humid topographically driven catchments with low permeability bedrock, shallow flow paths dominate and storage is small. Single or composite metrics such as flow path length or gradient tend to scale with catchment MTT since landscape form acts as a sufficient proxy for the subsurface mixing volume (McGlynn et al., 2003; McGuire et al., 2005). However, as bedrock permeability increases and the active mixing zone deepens, storage likewise increases and simple topographic metrics no longer capture this, now much larger, storage volume that controls catchment MTT. Instead, metrics that are a better proxy for the increased subsurface storage are more suited. Hale and McDonnell (2016) compared catchments with similar rainfall-runoff regimes but with different underlying bedrock permeabilities. For less permeable younger catchments, MTT scaled with topographic characteristics, while MTT at older and more permeable catchments not only failed to scale with topographic characteristics but instead scaled to catchment area, indeed, a better proxy for the increased storage. This elegantly captured the effect of bedrock permeability, and thus storage, on catchment stream water age and the required shift in metrics to accurately reflect the increase in storage depth. In a further example, Asano and Uchida (2012) found that bedrock flow path depth controlled base flow MTT in eight nested granite catchments. Geologic structure was similar across all catchments, so that the volume of bedrock storage per unit area was set by the flow path depth. Accordingly, flow path depth accurately scaled with subsurface storage volume and thus differences in catchment MTT between catchments.

At Maimai, bedrock groundwater age was not captured by topographic metrics likely because these metrics fail to capture the larger three-dimensional flow domain and storage volume that determined groundwater age. However, it should be pointed out that Maimai streamflow is dominated by shallow subsurface flow paths, thus simple landscape-derived metrics should scale to stream water MTT at this site. Indeed, this was found in earlier studies at Maimai by McGlynn et al. (2003). In general, as catchments shift from shallower to deeper flow path dominance, the metrics that capture discharge MTT should equally shift to capture the increasing volume of storage, which acts as a primary control on setting mean catchment age (Pfister et al., 2017).

5.3. Stream Water Transit Times Dominated by Contrasting Shallow and Young Soil Water Versus Deep and Old Bedrock Groundwater

Our silica-based TT estimates demonstrate the time-varying nature of stream water TT at M8. This highlights the intricate connection between catchment wetness condition, discharge, and transit time. Antecedent wetness conditions and event precipitation drive spatially distributed landscape scale connectivity that determines the release of differentially aged water from differentially stored subsurface units to the stream channel. The integration of these varying runoff sources through time and space form the single time-varying mean runoff age observed at the catchment outlet (Soulsby et al., 2015). The contrasting seasonal nature of stream water TT at M8 reflects seasonal shifts in environmental forcing factors, primarily precipitation, and evapotranspiration, which drive landscape scale shifts in hydrologic connectivity. The Maimai remained under high wetness conditions for nearly 8 months of the year from March to October, and correspondingly, young shallow subsurface flow dominated runoff. Stream water TT remained near 4 months, an age that corresponds to soil water storage residence times observed by Stewart and McDonnell (1991). During this extended wet period, TT was relatively stable and age fluctuations were minimal despite order-of-magnitude changes in catchment discharge. Perhaps most significant was the persistence of young stream water between storm events while the catchment drained. Elevated base flow discharge, sourced primarily from younger soil water storage, dominated runoff, and diluted the older bedrock groundwater discharge signal.

During summer months, when precipitation inputs dropped slightly and evapotranspiration rates increased significantly, base flow decreased by almost 3 orders of magnitude compared to the wet season. Antecedent wetness was low and spatial connectivity of shallow soil stores to the stream channel declined. Stream water TT became highly variable. Transient connectivity of younger shallow flow paths during and immediately following rain events temporarily changed stream water to much shorter TTs. But between events TT lengthened considerably, reflecting the contraction of younger flow paths and the reduction of discharge volume to levels where contributions from older bedrock groundwater were proportionately more significant.

Birkel et al. (2015) similarly found antecedent wetness drove hydrologic connectivity at a Scottish Highlands catchment, which in turn also controlled the time-varying nature of stream water TT. Interestingly, their TT time series, established using a tracer-aided model, showed an almost reverse trend from what we found at M8 (Soulsby et al., 2015): TT was stable at low discharge and highly dynamic (and young) at high discharge. This contrast from Maimai perhaps offers end-member examples of differences in catchment storage and the resulting transit time dynamics that arise from differences in shallow-versus-deep proportioning of subsurface water in humid catchments. At the "more permeable" Scottish catchment (with its glacial drift deposits and deep soils), greater volumes of catchment precipitation are transferred to deeper storage, and accordingly, runoff contains greater contributions of this storage unit across all flow conditions. This deep storage acts as the primary source of runoff during low flows and stream water TTs reflect the age of this single stable storage unit. At higher flows, although younger flow paths are activated, they do not completely inundate the dominant deeper groundwater signal and catchment TT is controlled by the proportional mixing of the two (or more) storage units. This creates a highly flow dependent and highly variable stream water TT at higher flows. But at Maimai, where the redistribution of moisture to deep groundwater storage is minimal, the reverse dynamics were observed. Stream water TT is stable at high flows, reflective of the large volume of young shallow water effusing to the stream channel that effectively "drowns out" the bedrock groundwater signal (Figure 7). However, during low-flow periods bedrock groundwater contributions, although small, are proportionately significant and stream water TT becomes highly variable with large age fluctuations across a small range of discharge. Differences in subsurface permeability contrasts between these two sites drive different patterns of subsurface moisture redistribution, so while stream water TT is controlled by the proportional mixing of the two main catchment storage units at both catchments, the conditions under which these storages dominate streamflow are reversed.

These results are in line with recent theoretical analysis of Berghuijs and Kirchner (2017) who explained the general, but somewhat paradoxical observation, of young rivers draining old aquifers. Under steady state conditions they showed that the mean age of water residing in an aquifer could be much older than the mean age of water discharging from that aquifer. This age contrast was directly controlled by contrasts in hydraulic conductivity within a hypothetical two-layered aquifer system. The M8 subsurface structure, where shallow highly conductive soil sits atop deep and much less permeable bedrock provides a clear and compelling field-based example that supports this theoretical work. Indeed, mean stream water transit times on the order of months contrast ages of bedrock groundwater that extend to multiple decades. Although our groundwater age observations do not provide a mean age of the entire aquifer, the spatial sampling of this aquifer by our 40 wells provides some insight, if only qualitatively, to the distribution of ages within the groundwater system (in our data, 0.1–23 years). It is clear that large volumes of the hillslope bedrock aquifer are much older than the surface water system they drain into. This supports other recent observations of isolated groundwater systems and the preferential release of younger stored water (Berghuijs & Kirchner, 2017; Jasechko et al., 2016, 2017).

5.4. An Evolving Perceptual Model of Maimai Hydrology

Previous water balance studies at the site concluded that the bedrock underlying Maimai was "essentially impermeable" (Pearce et al., 1977), a notion adopted by subsequent studies (McDonnell, 1990; McGlynn et al., 2002; O'Loughlin et al., 1978) and embedded into the evolving perceptual rainfall-runoff model for nearly 40 years despite no actual testing of the bedrock itself. The Pearce et al. (1977) water balance suggested that water loss to the deeper groundwater system was only 100 mm/yr, yet measured hillslope runoff ratios of only $\sim$13% (Woods & Rowe, 1996) contrasted with a catchment scale runoff ratio of nearly 60% (Pearce et al., 1977). These contradictory observations hinted at loss of subsurface hillslope stormflow to the bedrock and potential riparian zone subsidies of water from these deeper hillslope flow pathways. More recent bedrock testing at Maimai revealed bedrock saturated hydraulic conductivities that questioned initial claims of "impermeability" (Graham et al., 2010), with bedrock groundwater dynamics observed on storm-event time scales (Gabrielli et al., 2012). This has suggested a deeper hydrologically active zone than previously thought.

So why have previous studies at Maimai not seen bedrock groundwater? Simply put, bedrock groundwater contributions to streamflow at Maimai are extremely limited. Figure 8 shows our conceptual model of the primary groundwater flow paths and general groundwater flow domain. The lack of fractured bedrock, low bedrock conductivity, and predominately downward hydraulic gradients result in a relatively isolated groundwater body that has limited connectivity to the stream channel. Further, the sharp permeability contrast at the soil-bedrock interface causes most infiltrating water to flow laterally downslope at this boundary instead of continuing vertically into the bedrock. This, combined with shallow soils, minimal available soil storage, and long periods of high antecedent wetness means that the majority of precipitation flows only through the soil profile en route to the stream channel resulting in the now well-observed high runoff ratios, large volumes of quick flow, and young runoff observed at Maimai (McDonnell, 1990; Mosley, 1979; Pearce et al., 1986).

Although bedrock groundwater storage (based on porosity and volume of saturated bedrock) is large at M8, the low bedrock hydraulic conductivity results in a minimal groundwater flux within the headwater aquifer. This has the effect of increasing the bedrock groundwater age, while simultaneously reducing contributions to the stream channel. So although the potential of bedrock groundwater to influence stream

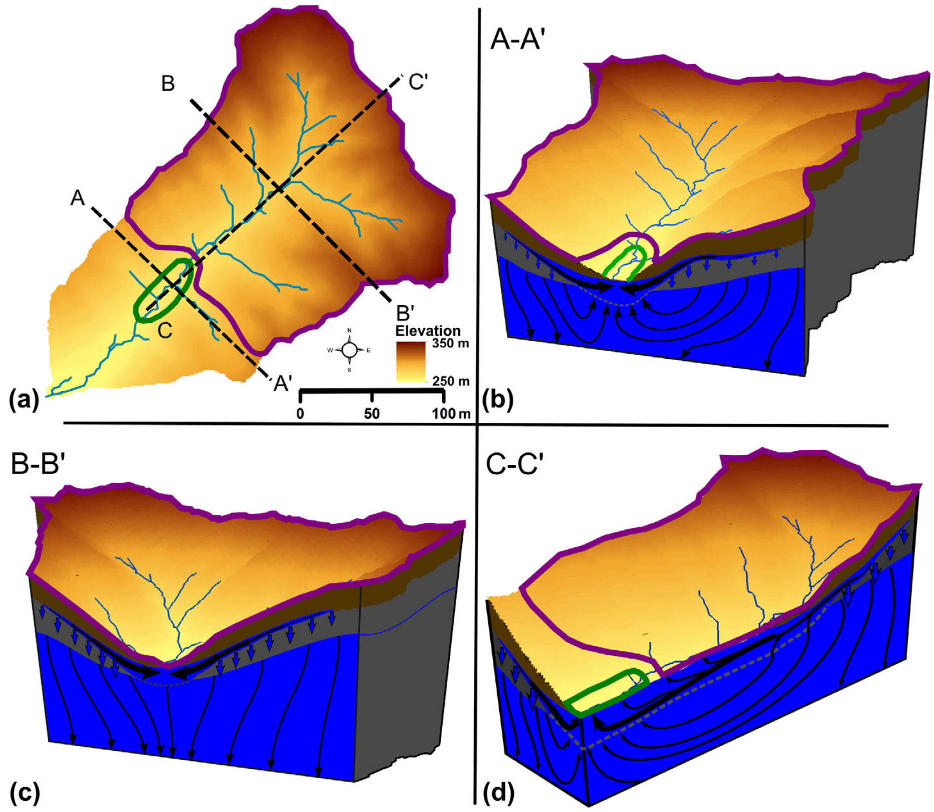

Figure 8. Perceptual model of the bedrock groundwater flow domain through various cross sections of the M8 catchment. (a) shows approximate area of observed bedrock groundwater recharge and discharge zones represented by the magenta and green outline, respectively. Cross section A-A′ (b) shows deeper and older contributions of bedrock groundwater discharge to the lower reach of the stream channel with some portion of hillslope recharge being lost to the larger regional groundwater system. Cross section B-B′ (c) shows groundwater recharge occurring across all landscape positions in the upper portion of the catchment, and cross section C-C′ (d) displays the upper reaches of the riparian zone contributing soil water to bedrock groundwater recharge and to stream discharge, while the lower reach of the riparian zone contributes both hillslope-derived soil water and bedrock groundwater to the stream.

water TT is high because its age is much greater than that of other shallower storages, this is offset by the low total bedrock discharge volume—which is too small to considerably alter stream water MTT under most runoff conditions. This dichotomy establishes what is effectively a two-storage compartmentalized hydrologic system with a young, shallow, and dominant upper domain and a much deeper and relatively isolated older groundwater body beneath.

Lastly, it is necessary to address the conflicting hillslope versus catchment runoff ratios that initially led to the notion of a hillslope bedrock underflow runoff mechanism. Upon further inspection, the 110 day hillslope monitoring period conducted by Woods and Rowe (1996) at Maimai occurred during the summer months when high evapotranspiration and reduced precipitation had dried up the catchment. This had the effect of increasing the necessary precipitation input to surpass hillslope runoff generation thresholds, and thus, many small storms produced no hillslope runoff. This caused the hillslope runoff ratio during this period to dramatically deviate from the annually averaged total catchment runoff ratio.

Although event-scale water table dynamics were observed within the bedrock aquifer both during our study and previously (Gabrielli et al., 2012), they are likely an integrated response to changes in barometric pressure (Van der Kamp & Gale, 1983), precipitation-induced pressure propagation (Rasmussen, 2001; Rigon et al., 2016), and small amounts of direct recharge to the water table. In the steep landscape at Maimai, increases in water table height over both storm and seasonal time scales do not equate to proportionally large changes in groundwater hydraulic head. For example, a midslope water table may rise 0.2 m during a large storm event, however, if this position were 30 m above the riparian zone, the resulting hydraulic gradient change would be only 0.7%. In unfractured low-conductivity bedrock, this would not alter considerably the groundwater flow structure, and no measurable increase in bedrock groundwater discharge would likely occur. Although, small rises in water table can produce large volumes of hillslope discharge in shallow soils due to a transmissivity feedback mechanism (Bishop et al., 2004), we do not expect this phenomena to occur within the deeper bedrock underlying Maimai.

Early water balance estimates at Maimai by Pearce et al. (1977) calculated approximately 100 mm/yr loss to deeper groundwater. In a system which receives 2,600 mm of rainfall annually and has minimal groundwater flux, small uncertainties inherent in precipitation, discharge, and evapotranspiration measurements can be equal to the total estimated loss to deeper groundwater. We are therefore cautious to place an exact value on bedrock groundwater recharge and discharge amounts. However, our new analysis suggests that approximately 200 mm/yr is recharged to the bedrock aquifer, half of which is discharged back into the catchment above the M8 weir and thus contributes to runoff generation processes, while the other half likely subsidizes flows at larger catchment scales down valley from the upper M8 headwaters (the subject of active ongoing work).

6. Conclusion

Our findings showed that despite a relatively shallow bedrock groundwater aquifer that displayed both event and seasonal scale water table fluctuations, bedrock groundwater contributions to catchment discharge at Maimai were minimal. The unfractured low-conductivity bedrock limits percolation to depth over short periods of time, and therefore, bedrock groundwater infiltration was controlled by the permeability of the bedrock matrix, occurring as flow through the primary porosity of the conglomerate bedrock. Although bedrock groundwater storage itself was considerable, the low recharge rate combined with the stable hillslope water tables likely drives an annually constant discharge to the riparian corridor. With the exception of some transient event-scale switches in vertical groundwater gradient at two well locations, the general gradient direction remained temporally and spatially constant throughout all conditions. All hillslope locations and mid and upper reaches of the riparian zone were groundwater sinks, while a small zone of upwelling bedrock groundwater was identified near the catchment outlet.

We noted a shift from soil storage effusion during the 8 month wet season to a combined soil and bedrock storage effusion during the drier summer months, which was reflected in stream water MTT. During the wet season, large volumes of young soil water controlled the stream water MTT signal and maintained a relatively stable and young stream water age even during interstorm periods. During drier months, bedrock groundwater contributions to runoff became proportionally large enough to exert some control on stream water MTT. During these intervals, stream age fluctuates significantly between young and old conditions corresponding to storm and interstorm periods and reflected the mixing of the two main catchment storage units.

Acknowledgments
This work was supported through funding by NSERC Discovery grant to J.J. McDonnell and the Horton Hydrology Research Grant from the American Geophysical Union to Christopher Gabrielli. We thank John Payne at Landcare Research, Matt Taylor, Christie Thomson, Emma and Bob Noonan, and Shaun and Jacqui McCracken for their invaluable assistance and support in the field and throughout the extended field campaign in New Zealand. No real or perceived financial or personal conflicts of interests exist for any author. Data supporting the conclusions can be obtained within references and tables where appropriate, and through this DOI: https://doi.org/10.17605/OSF.IO/B62KC. We thank the three reviewers for helping strengthen the final manuscript.

References

Anderson, S. P., Dietrich, W. E., Montgomery, D. R., Torres, R., Conrad, M. E., & Loague, K. (1997). Subsurface flow paths in a steep, unchanneled catchment. *Water Resources Research*, *33*(12), 2637–2653.

Asano, Y., & Uchida, T. (2012). Flow path depth is the main controller of mean base flow transit times in a mountainous catchment. *Water Resources Research*, *48*, W03512. https://doi.org/10.1029/2011WR010906

Asano, Y., Uchida, T., Mimasu, Y., & Ohte, N. (2009). Spatial patterns of stream solute concentrations in a steep mountainous catchment with a homogeneous landscape. *Water Resources Research*, *45*, W10432. https://doi.org/10.1029/2008WR007466

Asano, Y., Uchida, T., & Ohte, N. (2002). Residence times and flow paths of water in steep unchanneled catchments, Tanakami, Japan. *Journal of Hydrology*, *261*(1–4), 173–192. https://doi.org/10.1016/S0022-1694(02)00005-7

Berghuijs, W. R., & Kirchner, J. W. (2017). The relationship between contrasting ages of groundwater and streamflow. *Geophysical Research Letters*, *44*, 8925–8935. https://doi.org/10.1002/2017GL074962

Beven, K. J., & Kirkby, M. J. (1979). A physically based, variable contributing area model of basin hydrology. *Hydrological Sciences Bulletin*, *24*(1), 43–69.

Binley, A., Cassiani, G., & Deiana, R. (2010). Hydrogeophysics: Opportunities and challenges. *Bollettino di Geofisica Teorica ed Applicata*, *51*(4), 267–284.

Birkel, C., Soulsby, C., & Tetzlaff, D. (2015). Conceptual modelling to assess how the interplay of hydrological connectivity, catchment storage and tracer dynamics controls nonstationary water age estimates. *Hydrological Processes*, *29*(13), 2956–2969.

Bishop, K., Seibert, J., Köhler, S., & Laudon, H. (2004). Resolving the double paradox of rapidly mobilized old water with highly variable responses in runoff chemistry. *Hydrological Processes*, *18*(1), 185–189.

Bowen, F. (1967). Early Pleistocene glacial and associated deposits of the West Coast of the South Island, New Zealand. *New Zealand Journal of Geology and Geophysics*, *10*(1), 164–181.

Brammer, D. (1996). *Hillslope hydrology in a small forested catchment, Maimai, New Zealand* (MS Thesis). Syracuse, NY: State University of New York College of Environmental Science and Forestry.

Brooks, R., Barnard, H., Coulombe, R., & Mcdonnell, J. (2010). Two water worlds paradox: Trees and streams return different water pools to the hydrosphere. *Nature Geoscience*, *3*, 100–104.

Burns, D. A., Plummer, L. N., McDonnell, J. J., Busenberg, E., Casile, G. C., Kendall, C., et al. (2003). The geochemical evolution of riparian ground water in a forested piedmont catchment. *Ground Water*, *41*(7), 913–925.

Clark, M. P., Kavetski, D., & Fenicia, F. (2011). Pursuing the method of multiple working hypotheses for hydrological modeling. *Water Resources Research*, *47*, W09301. https://doi.org/10.1029/2010WR009827

Creutzfeldt, B., Troch, P. A., Güntner, A., Ferré, T. P. A., Graeff, T., & Merz, B. (2014). Storage-discharge relationships at different catchment scales based on local high-precision gravimetry. *Hydrological Processes*, *28*(3), 1465–1475. 10.1002/hyp.9689

Ebel, B. A., & Loague, K. (2006). Physics-based hydrologic-response simulation: Seeing through the fog of equifinality. *Hydrological Processes*, *20*(13), 2887–2900. 10.1002/hyp.6388

Edmunds, W., & Smedley, P. (2000). Residence time indicators in groundwater: The East Midlands Triassic sandstone aquifer. *Applied Geochemistry*, *15*(6), 737–752.

Fetter, C. W. (2000). *Applied hydrogeology*. Upper Saddle River, NJ: Prentice Hall.

Freeze, R. A., & Cherry, J. A. (1979). *Groundwater*. Englewood Cliffs, NJ: Prentice-Hall.

Fujimoto, M., Kosugi, K. I., Tani, M., Banba, N., & Fukagawa, R. (2014). Evaluation of bedrock groundwater movement in a weathered granite hillslope using tracer methods. *International Journal of Erosion Control Engineering*, *7*(1), 32–40. https://doi.org/10.13101/ijece.7.32

Gabrielli, C. P., & McDonnell, J. J. (2012). An inexpensive and portable drill rig for bedrock groundwater studies in headwater catchments. *Hydrological Processes*, *26*(4), 622–632. https://doi.org/10.1002/hyp.8212

Gabrielli, C. P., McDonnell, J. J., & Jarvis, W. T. (2012). The role of bedrock groundwater in rainfall-runoff response at hillslope and catchment scales. *Journal of Hydrology*, *450*, 117–133. https://doi.org/10.1016/j.jhydrol.2012.05.023

Gleeson, T., & Manning, A. H. (2008). Regional groundwater flow in mountainous terrain: Three-dimensional simulations of topographic and hydrogeologic controls. *Water Resources Research*, *44*, W10403. https://doi.org/10.1029/2008WR006848

Gleeson, T., Novakowski, K., & Kurt Kyser, T. (2009). Extremely rapid and localized recharge to a fractured rock aquifer. *Journal of Hydrology*, *376*(3–4), 496–509. https://doi.org/10.1016/j.jhydrol.2009.07.056

Graham, C. B., Woods, R. A., & McDonnell, J. J. (2010). Hillslope threshold response to rainfall: (1) A field based forensic approach. *Journal of Hydrology*, *393*(1–2), 65–76. https://doi.org/10.1016/j.jhydrol.2009.12.015

Grant, G. E., & Dietrich, W. E. (2017). The frontier beneath our feet. *Water Resources Research*, *53*, 2605–2609. https://doi.org/10.1002/2017WR020835

Haitjema, H. M., & Mitchell-Bruker, S. (2005). Are water tables a subdued replica of the topography? *Ground Water*, *43*(6), 781–786. https://doi.org/10.1111/j.1745-6584.2005.00090

Hale, V. C., & Mcdonnell, J. J. (2016). Effect of bedrock permeability on stream base flow mean transit time scaling relations: 1. A multiscale catchment intercomparison. *Water Resources Research*, *52*, 1358–1374. https://doi.org/10.1002/2014WR016124

Hale, V. C., McDonnell, J. J., Stewart, M. K., Solomon, D. K., Doolitte, J., Ice, G. G., et al. (2016). Effect of bedrock permeability on stream base flow mean transit time scaling relationships: 2. Process study of storage and release. *Water Resources Research*, *52*, 1375–1397. https://doi.org/10.1002/2015WR017660

Haria, A. H., & Shand, P. (2004). Evidence for deep sub-surface flow routing in forested upland Wales: Implications for contaminant transport and stream flow generation. *Hydrology and Earth System Sciences Discussions*, *8*(3), 334–344.

Harman, C. J. (2015). Time-variable transit time distributions and transport: Theory and application to storage-dependent transport of chloride in a watershed. *Water Resources Research*, *51*, 1–30. https://doi.org/10.1002/2014WR015707

Harr, R. D. (1977). Water flux in soil and subsoil on a steep forested slope. *Journal of Hydrology*, *33*, 37–58.

Hewlett, J. D., & Hibbert, A. R. (1967). Factors affecting the response of small watersheds to precipitation in humid areas. In Sopper, W. E. & Lull, H. W. (Eds.), *Forest hydrology* (pp. 275–291). New York, NY: Pergamon Press.

Hvorslev, M. J. (1951). *Time lag and soil permeability in ground-water observations*. Vicksburg, MS: U.S. Army Waterways Experiment Station.

Iwagami, S., Tsujimura, M., Onda, Y., Shimada, J., & Tanaka, T. (2010). Role of bedrock groundwater in the rainfall-runoff process in a small headwater catchment underlain by volcanic rock. *Hydrological Processes*, *24*(19), 2771–2783.

Jamieson, G. R., & Freeze, R. A. (1982). Determining hydraulic conductivity distributions in a mountainous area using mathematical modeling. *Ground Water*, *20*(2), 168–177.

Jasechko, S., Kirchner, J. W., Welker, J. M., & McDonnell, J. J. (2016). Substantial proportion of global streamflow less than three months old. *Nature Geoscience*, *9*(2), 126–129. https://doi.org/10.1038/ngeo2636

Jasechko, S., Perrone, D., Befus, K. M., Cardenas, M. B., Ferguson, G., Gleeson, T., et al. (2017). Global aquifers dominated by fossil groundwaters but wells vulnerable to modern contamination. *Nature Geoscience*, *10*(6), 425–429.

Katsura, S. Y., Kosugi, K. I., Mizutani, T., Okunaka, S., & Mizuyama, T. (2008). Effects of bedrock groundwater on spatial and temporal variations in soil mantle groundwater in a steep granitic headwater catchment. *Water Resources Research*, *44*, W09430. https://doi.org/10.1029/2007WR006610

Katsura, S. Y., Kosugi, K. I., Yamakawa, Y., & Mizuyama, T. (2014). Field evidence of groundwater ridging in a slope of a granite watershed without the capillary fringe effect. *Journal of Hydrology*, *511*, 703–718. http://doi.org/10.1016/j.jhydrol.2014.02.021

Katsuyama, M., Ohte, N., & Kabeya, N. (2005). Effects of bedrock permeability on hillslope and riparian groundwater dynamics in a weathered granite catchment. *Water Resources Research*, *41*, W01010. https://doi.org/10.1029/2004WR003275

Katsuyama, M., Tani, M., & Nishimoto, S. (2010). Connection between streamwater mean residence time and bedrock groundwater recharge/discharge dynamics in weathered granite catchments. *Hydrological Processes*, *24*(16), 2287–2299. https://doi.org/10.1002/hyp.7741

Katz, B. G., Chelette, A. R., & Pratt, T. R. (2004). Use of chemical and isotopic tracers to assess nitrate contamination and ground-water age, Woodville Karst Plain, USA. *Journal of Hydrology*, *289*(1–4), 36–61.

Kirchner, J. W. (2009). Catchments as simple dynamical systems: Catchment characterization, rainfall-runoff modeling, and doing hydrology backward. *Water Resources Research*, *45*, W02429. https://doi.org/10.1029/2008WR006912

Kohler, M. A., & Linsley, R. K. (1951). *Predicting the runoff from storm rainfall*. Washington, DC: US Department of Commerce, Weather Bureau.

Kosugi, K. I., Fujimoto, M., Katsura, S. Y., Kato, H., Sando, Y., & Mizuyama, T. (2011). Localized bedrock aquifer distribution explains discharge from a headwater catchment. *Water Resources Research*, *47*, W07530. https://doi.org/10.1029/2010WR009884

Kosugi, K. I., Katsura, S. Y., Katsuyama, M., & Mizuyama, T. (2006). Water flow processes in weathered granitic bedrock and their effects on runoff generation in a small headwater catchment. *Water Resources Research*, *42*, W02414. https://doi.org/10.1029/2005WR004275

Macdonald, L. H. (1988). An inexpensive, portable system for drilling into subsurface layers. *Soil Science Society of America Journal*, *52*, 1817–1819.
Małoszewski, P., & Zuber, A. (1982). Determining the turnover time of groundwater systems with the aid of environmental tracers: 1. Models and their applicability. *Journal of Hydrology*, *57*(3), 207–231.
Masaoka, N., Kosugi, K. I., Yamakawa, Y., & Tsutsumi, D. (2016). Processes of bedrock groundwater seepage and their effects on soil water fluxes in a foot slope area. *Journal of Hydrology*, *535*, 160–172. https://doi.org/10.1016/j.jhydrol.2016.01.081
Maxwell, R. M., & Condon, L. E. (2016). Connections between groundwater flow and transpiration partitioning. *Science*, *353*(6297), 377–380.
McDonnell, J., Mcguire, K., Aggarwal, P., Beven, K., Biondi, D., Destouni, G., et al. (2010). How old is streamwater? Open questions in catchment transit time conceptualization, modelling and analysis. *Hydrological Processes*, *24*(12), 1745–1754.
McDonnell, J. J. (1990). A rationale for old water discharge through macropores in a steep, humid catchment. *Water Resources Research*, *26*(11), 2821–2832.
McDonnell, J. J. (2017). Beyond the water balance. *Nature Geoscience*, *10*, 396.
McGlynn, B., McDonnell, J., Stewart, M., & Seibert, J. (2003). On the relationships between catchment scale and streamwater mean residence time. *Hydrological Processes*, *17*(1), 175–181.
McGlynn, B. L., & McDonnell, J. J. (2003). Role of discrete landscape units in controlling catchment dissolved organic carbon dynamics. *Water Resources Research*, *39*(4), 1090. https://doi.org/10.1029/2002WR001525
McGlynn, B. L., McDonnell, J. J., & Brammer, D. D. (2002). A review of the evolving perceptual model of hillslope flowpaths at the Maimai catchments, New Zealand. *Journal of Hydrology*, *257*, 1–26.
McGlynn, B. L., McDonnell, J. J., Seibert, J., & Kendall, C. (2004). Scale effects on headwater catchment runoff timing, flow sources, and groundwater-streamflow relations. *Water Resources Research*, *40*, W075041. https://doi.org/10.1029/2003WR002494
Mcguire, K., McDonnell, J., Weiler, M., Kendall, C., McGlynn, B., Welker, J., et al. (2005). The role of topography on catchment-scale water residence time. *Water Resources Research*, *41*, W05002. https://doi.org/10.1029/2004WR003657
McMillan, H. K., Clark, M. P., Bowden, W. B., Duncan, M., & Woods, R. A. (2011). Hydrological field data from a modeller's perspective: Part 1. Diagnostic tests for model structure. *Hydrological Processes*, *25*(4), 511–522.
McNamara, J. P., Tetzlaff, D., Bishop, K., Soulsby, C., Seyfried, M., Peters, N. E., et al. (2011). Storage as a metric of catchment comparison. *Hydrological Processes*, *25*(21), 3364–3371. https://doi.org/10.1002/hyp.8113
Millares, A., Polo, M. J., & Losada, M. A. (2009). The hydrological response of baseflow in fractured mountain areas. *Hydrology and Earth System Sciences*, *13*(7), 1261–1271. https://doi.org/10.5194/hess-13-1261-2009
Montgomery, D. R., Dietrich, W. E., Torres, R., Anderson, S. P., Heffner, J. T., & Loague, K. (1997). Hydrologic response of a steep, unchanneled valley to natural and applied rainfall. *Water Resources Research*, *33*(1), 91–109.
Morgenstern, U., Stewart, M. K., & Stenger, R. (2010). Dating of streamwater using tritium in a post nuclear bomb pulse world: Continuous variation of mean transit time with streamflow. *Hydrology and Earth System Sciences*, *14*(11), 2289–2301. https://doi.org/10.5194/hess-14-2289-2010
Morgenstern, U., & Taylor, C. B. (2009). Ultra low-level tritium measurement using electrolytic enrichment and LSC. *Isotopes in Environmental and Health Studies*, *45*(2), 96–117.
Mortimer, N., Sutherland, R., & Nathan, S. (2001). Torlesse greywacke and Haast Schist source for Pliocene conglomerates near Reefton, New Zealand. *New Zealand Journal of Geology and Geophysics*, *44*(1), 105–111.
Mosley, M. P. (1979). Streamflow generation in a forested watershed. *Water Resources Research*, *15*(4), 795–806.
Nathan, S., Anderson, H. J., Cook, R. A., Herzer, R., Hoskins, R., Raine, J., et al. (1986). *Cretaceous and Cenozoic sedimentary basins of the West Coast region, South Island, New Zealand*. New Zealand: Science Information Publishing Centre, DSIR, for the New Zealand Geological Survey.
Onda, Y., Komatsu, Y., Tsujimura, M., & Fujihara, J. I. (2001). The role of subsurface runoff through bedrock on storm flow generation. *Hydrological Processes*, *15*, 1693–1706.
O'loughlin, C. L., Rowe, L. K., & Pearce, A. J. (1978). Sediment yields from small forested catchments, North Westland-Nelson, New Zealand. *Journal of Hydrology*, *17*, 1–15.
Oshun, J., Dietrich, W. E., Dawson, T. E., & Fung, I. (2016). Dynamic, structured heterogeneity of water isotopes inside hillslopes. *Water Resources Research*, *52*, 164–189. https://doi.org/10.1002/2015WR017485
Overeem, A., Leijnse, H., & Uijlenhoet, R. (2013). Country-wide rainfall maps from cellular communication networks. *Proceedings of the National Academy of Sciences of the Unites States of America*, *110*(8), 2741–2745.
Pearce, A. J., O'loughlin, C. L., & Rowe, L. K. (1977). *Hydrologic regime of small, undisturbed beech forest catchments, north Westland*. New Zealand: Information Service, Department of Scientific and Industrial Research.
Pearce, A. J., & Rowe, L. K. (1979). Forest management effects on interception, evaporation, and water yield. *Journal of Hydrology*, *18*(2), 73–87.
Pearce, A. J., Stewart, M. K., & Sklash, M. G. (1986). Storm runoff generation in humid headwater catchments: 1. Where does the water come from? *Water Resources Research*, *22*(8), 1263–1272.
Penna, D., Meerveld, H., Oliviero, O., Zuecco, G., Assendelft, R., Dalla Fontana, G., & Borga, M. (2015). Seasonal changes in runoff generation in a small forested mountain catchment. *Hydrological Processes*, *29*(8), 2027–2042.
Peters, N. E., Burns, D. A., & Aulenbach, B. T. (2014). Evaluation of high-frequency mean streamwater transit-time estimates using groundwater age and dissolved silica concentrations in a small forested watershed. *Aquatic Geochemistry*, *20*(2–3), 183–202.
Pfister, L., Martínez-Carreras, N., Hissler, C., Klaus, J., Carrer, G. E., Stewart, M. K., et al. (2017). Bedrock geology controls on catchment storage, mixing and release: A comparative analysis of 16 nested catchments. *Hydrological Processes*, *31*, 1828–1845. https://doi.org/10.1002/hyp.11134
Praamsma, T., Novakowski, K., Kyser, K., & Hall, K. (2009). Using stable isotopes and hydraulic head data to investigate groundwater recharge and discharge in a fractured rock aquifer. *Journal of Hydrology*, *366*(1), 35–45.
Rantz, S. E. (1982). *Measurement and computation of streamflow: Volume 2, computation of discharge*. Washington, DC: United States Government Publishing Office.
Rasmussen, T. C. (2001). *Flow and transport through unsaturated fractured rock* (pp. 45–52). Washington, DC: American Geophysical Union.
Rempe D. M., & Dietrich W. E. (2018). Direct observations of rock moisture, a hidden component of the hydrologic cycle. *Proceedings of the National Academy of Sciences*. https://doi.org/10.1073/pnas.1800141115
Riebe, C. S., Hahm, W. J., & Brantley, S. L. (2017). Controls on deep critical zone architecture: A historical review and four testable hypotheses. *Earth Surface Processes and Landforms*, *42*(1), 128–156. https://doi.org/10.1002/esp.4052
Rigon, R., Bancheri, M., & Green, T. R. (2016). Age-ranked hydrological budgets and a travel time description of catchment hydrology. *Hydrology and Earth System Sciences*, *20*(12), 4929–4947. https://doi.org/10.5194/hess-20-4929-2016

Rinaldo, A., Benettin, P., Harman, C. J., Hrachowitz, M., Mcguire, K. J., Van Der Velde, Y., et al. (2015). Storage selection functions: A coherent framework for quantifying how catchments store and release water and solutes. *Water Resources Research*, *51*, 4840–4847. https://doi.org/10.1002/2015WR017273

Rowe, L., & Pearce, A. (1994). Hydrology and related changes after harvesting native forest catchments and establishing *Pinus radiata* plantations. Part 2. The native forest water balance and changes in streamflow after harvesting. *Hydrological Processes*, *8*(4), 281–297.

Salve, R., Rempe, D. M., & Dietrich, W. E. (2012). Rain, rock moisture dynamics, and the rapid response of perched groundwater in weathered, fractured argillite underlying a steep hillslope. *Water Resources Research*, *48*, W11528. https://doi.org/10.1029/2012WR012583

Salvucci, G. D., & Entekhabi, D. (1995). Hillslope and climatic controls on hydrologic fluxes. *Water Resources Research*, *31*(7), 1725–1739.

Sanford, W. (2002). Recharge and groundwater models: An overview. *Hydrogeology Journal*, *10*(1), 110–120. https://doi.org/10.1007/s10040-001-0173-5

Sayama, T., Mcdonnell, J. J., Dhakal, A., & Sullivan, K. (2011). How much water can a watershed store? *Hydrological Processes*, *25*, 3899–3908. https://doi.org/10.1002/hyp.8288

Seibert, J., Rodhe, A., & Bishop, K. (2003). Simulating interactions between saturated and unsaturated storage in a conceptual runoff model. *Hydrological Processes*, *17*(2), 379–390. https://doi.org/10.1002/hyp.1130

Sklash, M. G., Stewart, M. K., & Pearce, A. J. (1986). Storm runoff generation in humid headwater catchments: 2. A case study of hillslope and low-order stream response. *Water Resources Research*, *22*(8), 1273–1282.

Sophocleous, M. (2002). Interactions between groundwater and surface water: The state of the science. *Hydrogeology Journal*, *10*(1), 52–67.

Soulsby, C., Birkel, C., Geris, J., Dick, J., Tunaley, C., & Tetzlaff, D. (2015). Stream water age distributions controlled by storage dynamics and nonlinear hydrologic connectivity: Modeling with high-resolution isotope data. *Water Resources Research*, *51*, 7759–7776. https://doi.org/10.1002/2015WR017888

Sproles, E., Leibowitz, S., Reager, J., Wigington, P. Jr, Famiglietti, J., & Patil, S. (2015). GRACE storage-runoff hystereses reveal the dynamics of regional watersheds. *Hydrology and Earth System Sciences*, *19*(7), 3253. https://doi.org/10.5194/hess-19-3253-2015

Stewart, M. K., & McDonnell, J. J. (1991). Modeling base flow soil water residence times from deuterium concentrations. *Water Resources Research*, *27*, 2681–2693. https://doi.org/10.1029/91WR01569

Stewart, M. K., Mehlhorn, J., & Elliott, S. (2007). Hydrometric and natural tracer (oxygen-18, silica, tritium and sulphur hexafluoride) evidence for a dominant groundwater contribution to Pukemanga Stream, New Zealand. *Hydrological Processes*, *21*(24), 3340–3356.

Stewart, M. K., Morgenstern, U., Gusyev, M. A., & Maloszewski, P. (2017). Aggregation effects on tritium-based mean transit times and young water fractions in spatially heterogeneous catchments and groundwater systems. *Hydrology and Earth System Sciences*, *21*, 4615–4627. https://doi.org/10.5194/hess-21-4615-2017

Stocker, T. F. (2014). *Climate change 2013: The physical science basis: Working group I contribution to the fifth assessment report of the intergovernmental panel on climate change*. Cambridge, UK: Cambridge University Press.

Tague, C., & Grant, G. E. (2004). A geological framework for interpreting the low-flow regimes of Cascade streams, Willamette River Basin, Oregon. *Water Resources Research*, *40*, W04303. https://doi.org/10.1029/2003WR002629

Tetzlaff, D., Seibert, J., Mcguire, K., Laudon, H., Burns, D., Dunn, S., et al. (2009). How does landscape structure influence catchment transit time across different geomorphic provinces? *Hydrological Processes*, *23*(6), 945–953.

Todd, D. K. (1956). *Ground-water flow in relation to a flooding stream* (pp. 1–20). Reston, VI: American Society of Civil Engineers.

Uchida, T., & Asano, Y. (2010). Spatial variability in the flowpath of hillslope runoff and streamflow in a meso-scale catchment. *Hydrological Processes*, *24*(16), 2277–2286. https://doi.org/10.1002/hyp.7767

Uchida, T., Kosugi, K. I., & Mizuyama, T. (2002). Effects of pipe flow and bedrock groundwater on runoff generation in a steep headwater catchment in Ashiu, central Japan. *Water Resources Research*, *38*(7). https://doi.org/10.1029/2001WR000261

Van Der Kamp, G., & Gale, J. (1983). Theory of earth tide and barometric effects in porous formations with compressible grains. *Water Resources Research*, *19*(2), 538–544.

Voltz, T., Gooseff, M., Ward, A. S., Singha, K., Fitzgerald, M., & Wagener, T. (2013). Riparian hydraulic gradient and stream-groundwater exchange dynamics in steep headwater valleys. *Journal of Geophysical Research: Earth Surface*, *118*, 953–969. https://doi.org/10.1002/jgrf.20074

Wada Y., Van Beek L. P., Van Kempen C. M., Reckman J. W., Vasak S. & Bierkens M. F (2010). Global depletion of groundwater resources. *Geophysical Research Letters*, *37*(20). https://doi.org/10.1029/2010GL044571

Weiler, M., McGlynn, B. L., Mcguire, K. J., & McDonnell, J. J. (2003). How does rainfall become runoff? A combined tracer and runoff transfer function approach. *Water Resources Research*, *39*(11), 1315. https://doi.org/1310.1029/2003WR002331

White, T., Brantley, S., Banwart, S., Chorover, J., Dietrich, W., Derry, L., et al. (2015). The role of critical zone observatories in critical zone science. *Developments in Earth Surface Processes*, *19*, 15–78.

Winter, T. C., Rosenberry, D. O., & Labaugh, J. W. (2003). Where does the ground water in small watersheds come from? *Ground Water*, *41*(7), 989–1000.

Wittenberg H. & Sivapalan M. (1999). Watershed groundwater balance estimation using streamflow recession analysis and baseflow separation. *Journal of Hydrology*, *219*(1–2), 20–33.

Woods, R., & Rowe, L. (1996). The changing spatial variability of subsurface flow across a hillside. *Journal of Hydrology New Zealand*, *35*(1), 51–86.